Supplementary figures to

Tumor specific delivery of siRNA coupled superparamagnetic iron-oxide-nanoparticles, targeted against PLK1, stops progression of pancreatic cancer

Ujjwal M. Mahajan[1], Steffen Teller[1], Matthias Sendler[1], Raghavendra Palankar[2], Cindy van den Brandt[1], Theresa Schwaiger[1], Jens-Peter Kuehn[3], Silvia Ribback[4], Gunner Gloeckl[5], Matthias Evert[4], Werner Weitschies[5], Norbert Hosten[3], Frank Dombrowski[4], Mihaela Delcea[2], Frank-Ulrich Weiss[1], Markus M. Lerch[1#], Julia Mayerle[1#]

[1]Department of Medicine A, University Medicine, Ernst-Moritz-Arndt-University, Greifswald, Germany
[2]ZIK HIKE-Center for Innovation Competence, Humoral Immune Reactions in Cardiovascular Diseases, Greifswald, Germany,
[3]Department of Radiology and Neuroradiology, University Medicine, Ernst Moritz Arndt University Greifswald, Germany
[4]Institute of Pathology, University Medicine, Ernst-Moritz-Arndt-University, Greifswald, Germany
[5]Institute of Pharmacy, Ernst-Moritz-Arndt-University, Greifswald, Germany

Table S1: The physical characteristics of siPLK1-StAv-SPIONs, characterized using zetasizer to measure hydrodynamic diameter and zeta potential.

Hydrodynamic diameter is measure of particle core along dipole layers. Hydrodynamic particle diameter is mostly above the diameter of that measured with TEM or AFM because, when a dispersed particle moves through solution, electric dipole layer adheres to its surface and influences the movement of particles in solution.

Parameters	Z-Average (d. nm)	PDI	Zeta Potential (mV)
Dextran-SPIONs (SPIONs)	39 ± 9	0.25	-4.63
StAv-SPIONs	71 ± 18	0.29	-29.60
siPLK1-StAv-SPIONs	123 ± 14	0.21	-31.20
siPLK1 concentration	2.0672 ± 0.2692 µg/ml*		
siPLK1 concentration	2.0626 ± 0.6489 µg/ml$		
Entrapment Efficiency	30.08 ± 3.91%		
siPLK1 coupling per SPIONs	Approx. 5 siPLK1 per SPIONs#		

*calculated by RiboGreen RNA fluorescent quantification assay

$calculated by agarose gel electrophoresis followed by mean intensity calculation

calculated considering Avagadro's number and core SPIONs diameter

PDI: Polydispersity index

Table S2: The composition of siPLK1-StAv-SPIONs as determined by Energy-dispersive X-ray spectroscopy.

Element	Line Type	Apparent Concentration	k Ratio	Wt%	Wt% Sigma
C	K series	13.65	0.13645	**30.83**	0.37
O	K series	39.82	0.13399	**21.48**	0.23
Na	K series	0.38	0.00162	**0.36**	0.05
Cl	K series	5.66	0.04949	**2.56**	0.05
Fe	K series	92.77	0.92769	**44.76**	0.29
Total:				**100.00**	

Table S3: Table illustrating stoichiometric calculations for biotin binding sites, siRNA, MPAP and EPPT1.

Sr. No	Parameter	Unit value
1	Average diameter of SPION core (± SD)	9.81 ± 3.73nm
2.	Median diameter of SPION core (Range)	8.65nm (6.18 - 45.51nm)
3.	Average number of siRNAs/SPIONs	5
4.	Average number of EPPT1/SPIONs	16
5.	Average number of MPAP/SPIONs	21

Table S4: Table showing change in clinical serum parameters on the treatment ofsiPLK1-StAv-SPIONs in syngenic orthotopic tumor mice. siPLK1-StAv-SPIONs treatment did not show any significant deviation in serum markers corresponding to that of control.

Analyte	Units	Reference Values (MEAN ± SD)	Control			siPLK1				siControl-StAv-SPIONs				siPLK1-StAv-SPIONs			
			MEAN	SD	N	MEAN	SD	N	*P*	MEAN	SD	N	*P*	MEAN	SD	N	*P*
Glucose	mg/dl	247.0 ± 60.86	148.21	18.81	4	159.48	20.31	4	0.90	149.57	22.65	4	0.76	148.85	32.40	5	0.40
Creatinine	mg/dl	0.23 ± 0.12	0.14	0.01	4	0.14	0.01	4	1.00	0.15	0.01	4	0.28	0.14	0.01	5	0.92
BUN	mg/dl	14.34 ± 5.26	30.65	9.82	4	41.48	1.49	4	0.01	37.36	24.72	4	0.16	38.92	5.81	5	0.34
ALT	U/l	66.46 ± 184.87	21.90	16.34	4	50.55	34.33	4	0.25	23.70	15.01	4	0.89	43.44	15.37	5	0.87
AST	U/l	127.58 ± 142.05	103.50	33.36	4	206.10	216.74	4	0.01	97.20	98.83	4	0.11	144.00	33.94	5	1.00
Bilirubin	mg/dl	0.32 ± 0.28	0.12	0.02	4	0.13	0.06	4	0.18	0.10	0.01	4	0.05	0.10	0.01	5	0.08

BUN: blood urea nitrogen, AST; Aspartate aminotransferase, ALT: Alanine aminotransferase

* Reference values are from Charles-River laboratory C57BL/6N mice database

Table S5: Table showing changes in cytokine and chemokines on the treatment of siPLK1-StAv-SPIONs in syngenic orthotopic tumor mice. siPLK1-StAv-SPIONs treatment did not show any significant deviation in chemokines and cytokines levels corresponding to that of control

Cytokines in pg/ml	Control			siPLK1				siControl-StAv-SPIONs				siPLK1-StAv-SPIONs			
	MEAN	SD	N	MEAN	SD	N	*P*	MEAN	SD	N	*P*	MEAN	SD	N	*P*
IL12p70	2.92	2.34	4	120.47	183.72	4	0.26	1250.5	2151.59	4	0.06	396.38	600.68	4	0.03
TNFα	4.94	3.37	4	10.03	4.43	4	0.11	9.97	12.36	4	1.00	7.47	4.12	4	0.48
IFNɣ	0.36	0.33	4	1.61	0.67	4	0.03	26.53	44.68	4	0.23	4.12	5.58	4	0.13
MCP1	25.22	12.16	4	33.42	6.88	4	0.34	46.13	48.01	4	0.63	28.48	15.98	4	0.89
IL10	2.60	4.51	4	26.09	31.95	4	0.30	391.84	634.87	4	0.11	98.79	158.81	4	0.30
IL6	15.44	14.32	4	160.33	279.49	4	0.85	125.04	213.40	4	1.00	44.69	65.95	4	0.88

Table S6: Table showing change in clinical Hematology parameters (Whole Blood Count) and health status on the treatment ofsiPLK1-StAv-SPIONs in C57BL/6N mice. siPLK1-StAv-SPIONs treatment did not show any significant deviation corresponding to control, However, BI6727 showed classical side effects associated with PLK1 inhibition.

Analyte	Units	Reference values (MEAN ± SD)	Control (n=10)		BI6727 (n=10)			siControl-StAv-SPIONs (n=10)			siPLK1-StAv-SPIONs (n=8-10)		
			MEAN	SD	MEAN	SD	*P*	MEAN	SD	*P*	MEAN	SD	*P*
Change in Body Weight													
	%		1.29	2.97	17.10	5.08	*0.00*	0.58	2.48	*0.65*	1.68	2.21	*0.51*
Haematology													
WBCs	K/µl	8.91 ± 2.5	7.73	1.72	4.41	1.20	*0.00*	9.84	3.70	*0.12*	7.10	1.55	*0.40*
Erythrocytes	M/µl	9.51 ± 1.25	10.25	0.65	9.17	0.70	*0.00*	8.29	1.15	*0.00*	9.16	0.88	*0.01*
Haemoglobin	g/dl	14.33 ± 2.64	14.71	0.81	12.92	1.20	*0.00*	11.62	1.53	*0.00*	12.87	1.20	*0.00*
Haematocrit	%	47.02 ± 7.27	54.63	3.90	48.33	3.58	*0.00*	45.66	4.91	*0.00*	48.60	4.21	*0.00*
MCH	pg	14.88 ± 1.03	14.37	0.34	14.11	0.27	*0.06*	14.08	0.61	*0.19*	14.08	0.40	*0.09*
MCV	fL	49.44 ± 3.95	53.27	1.67	52.80	1.35	*0.49*	55.51	3.26	*0.07*	53.17	1.22	*0.88*
MCHC	g/dl	30.28 ± 3.04	26.96	0.57	26.72	0.91	*0.48*	25.39	0.97	*0.00*	26.51	0.69	*0.12*
RDW	%	17.89 ± 1.15	22.32	1.38	21.17	1.31	*0.07*	24.23	3.32	*0.11*	22.43	1.56	*0.86*
Platelets	K/µl	1350.67 ± 337.98	957.20	171.50	783.70	248.88	*0.05*	1059.10	137.10	*0.15*	1026.80	128.89	*0.31*
MPV	fL	5.04 ± 0.44	6.71	0.26	6.94	0.33	*0.10*	6.67	0.25	*0.80*	6.74	0.29	*0.72*
Eosinophils	K/µl	0.14 ± 0.12	0.00	0.00	0.00	0.00	*ND*	0.00	0.00	*ND*	0.00	0.00	*ND*
Basophils	K/µl	0.03 ± 0.03	0.02	0.01	0.01	0.01	*0.11*	0.02	0.02	*0.94*	0.02	0.01	*0.43*
Neutrophils	K/µl	1.45 ± 1.01	0.57	0.24	0.21	0.22	*0.00*	0.99	0.66	*0.01*	0.72	0.36	*0.32*
Lymphocytes	K/µl	6.85 ± 1.97	7.11	1.72	3.33	2.13	*0.00*	8.42	3.06	*0.25*	6.54	1.45	*0.47*
Monocytes	K/µl	0.43 ± 0.24	0.02	0.02	0.05	0.07	*0.37*	0.42	0.43	*0.02*	0.07	0.05	*0.06*
Normoblasts	K/µl	0.01 ± 0.01	0.02	0.01	0.07	0.12	*0.17*	0.02	0.04	*0.83*	0.04	0.03	*0.16*
Health status													
Body Conditioning score (BCS)			2.80	0.22	2.30	0.35	*0.00*	2.77	0.15	*0.89*	2.87	0.16	*0.32*
Individiual behaviour			0.20	0.40	0.60	0.49	*0.08*	0.30	0.46	*0.63*	0.00	0.00	*0.22*
Stance			0.00	0.00	0.20	0.40	*0.22*	0.00	0.00	*1.00*	0.00	0.00	*1.00*
Haircoat			0.30	0.46	1.10	0.83	*0.03*	0.30	0.46	*1.00*	0.20	0.40	*0.63*
Position of eyes			0.20	0.40	0.30	0.46	*0.63*	0.20	0.40	*1.00*	0.20	0.40	*1.00*
Discharge from eye or nose			0.00	0.00	0.00	0.00	*1.00*	0.20	0.40	*0.22*	0.10	0.30	*0.46*
Cleanliness of anal orifice			0.20	0.40	0.20	0.60	*0.66*	0.00	0.00	*0.22*	0.20	0.40	*1.00*
Condition of tail			0.00	0.00	0.10	0.30	*0.46*	0.20	0.40	*0.22*	0.30	0.46	*0.10*
Condition of paws and ears			0.10	0.30	0.40	0.49	*0.15*	0.10	0.30	*1.00*	0.00	0.00	*0.46*
Palpation			0.00	0.00	0.90	0.70	*0.00*	0.10	0.30	*0.46*	0.20	0.40	*0.22*

MCH: mean corpuscular haemoglobin, MCV:mean corpuscular volume, MCHC: mean corpuscular haemoglobin concentration, RDW: red blood cell distribution width, MPV: mean platelet volume

BCS: 1-5, 1 being emacicated and 5 being Obese

Other health status score: 0 to 3, 0 being normal and 3 being severe abnormality

Reference values are from Charles-River laboratory C57BL/6N mice database

Table S7: Pharmacokinetic profiling of siPLK1-StAv-SPIONs showed a plasma half life of 208 min with a mean plasma residual time of 292 min.

Parameter	Unit	MEAN	SEM	N
Lambda_z	1/min	0.0048	0.000757	5
t1/2	**min**	**208.1891**	**22.55904**	**5**
Tmax	**min**	**3.4**	**0.178885**	**5**
Cmax	mg/L	34.67811	2.074008	5
C0	mg/L	51.65142	6.370483	5
Clast_obs/Cmax		0.112462	0.016859	5
AUC 0-t	mg/L*min	3155.759	210.2443	5
AUC 0-inf_obs	mg/L*min	4223.871	283.0248	5
AUC 0-t/0-inf_obs		0.768829	0.026548	5
AUMC 0-inf_obs	mg/L*min^2	1359200	162994.8	5
MRT 0-inf_obs	**min**	**292.1614**	**32.51097**	**5**
Vz_obs	(mg/kg)/(mg/L)	0.184009	0.014101	5
Cl_obs	(mg/kg)/(mg/L)/min	0.000743	8.55E-05	5
vss_obs	(mg/kg)/(mg/L)	0.17465	0.015522	5

Lambda_z: Terminal elimination rate constant, **t1/2:** Half-life, **Tmax:** Time to reach maximum concentration, **Cmax:** Concentration at Tmax, **C0:** Concentration without distribution, **Clast_obs/Cmax:** Last observed concentration, **AUC 0-t:** Area under curve from 0 to Clast_obs, **AUC 0-inf_obs:** Area under curve from 0 to infinity, **AUC 0-t/0-inf_obs AUMC 0-inf_obs:** Area under first moment curve, **MRT 0-inf_obs:** Mean residual time, **Vz_obs:** Volume of distribution at terminal state, **Cl_obs:** Total clearance, **vss_obs:** Volume of distribution at steady state

Table S8: Table showing change in clinical serum parameters on the treatment ofsiPLK1-StAv-SPIONs in tumor bearing KPC mice. siPLK1-StAv-SPIONs treatment did not show any significant deviation in serum markers corresponding to that of control

Analyte	Units	Reference Values (MEAN ± SD)	StAv-SPIONs			siControl-StAv-SPIONs				siPLK1-StAv-SPIONs			
			MEAN	SD	N	MEAN	SD	N	*P*	MEAN	SD	N	P
Glucose	mg/dl	247.0 ± 60.86	76.13	22.23	4	69.08	28.74	3	0.73	64.27	27.99	3	0.56
Creatinine	mg/dl	0.23 ± 0.12	<0.15	0.00	4	<0.15	0.00	4	ND	<0.15	0.00	4	ND
BUN	mg/dl	14.34 ± 5.26	26.69	4.68	4	35.18	17.41	3	0.38	27.86	5.18	3	0.77
ALT	U/l	66.46 ± 184.87	0.60	0.49	4	16.60	28.23	3	0.29	0.80	0.34	3	0.58
AST	U/l	127.58 ± 142.05	24.90	7.85	4	248.40	357.67	3	0.35	43.20	7.86	3	0.05
Bilirubin	mg/dl	0.32 ± 0.28	<0.10	0.00	4	<0.10	0.00	4	ND	<0.10	0.00	4	ND

BUN: blood urea nitrogen, AST; Aspartate aminotransferase, ALT: Alanine aminotransferase

*Below Detection Level

ND: Not detected

Reference values are from Charles-River laboratory C57BL/6N mice database

(a)

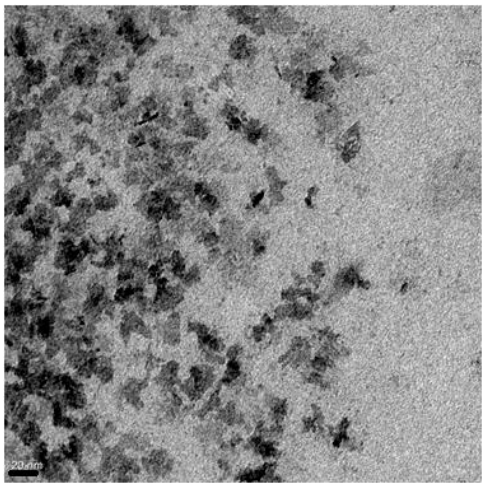

(b)

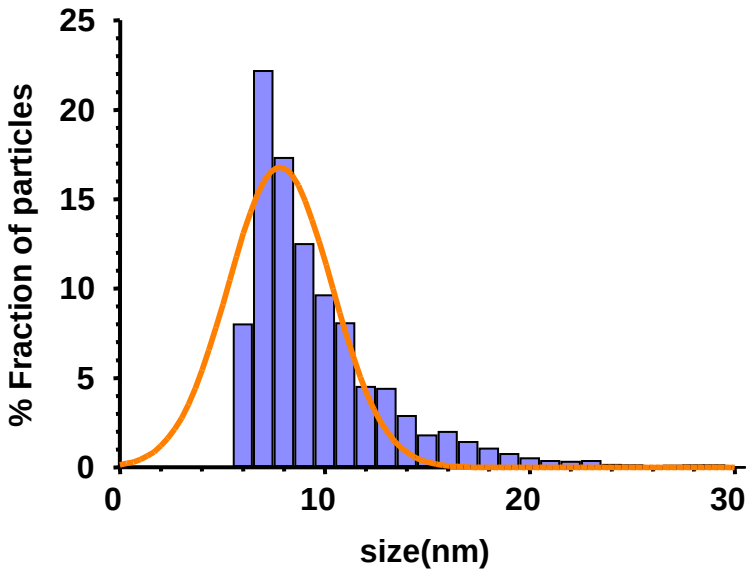
% Fraction of particles
size(nm)
0
5
10
15
20
25
0
10
20
30

(c)

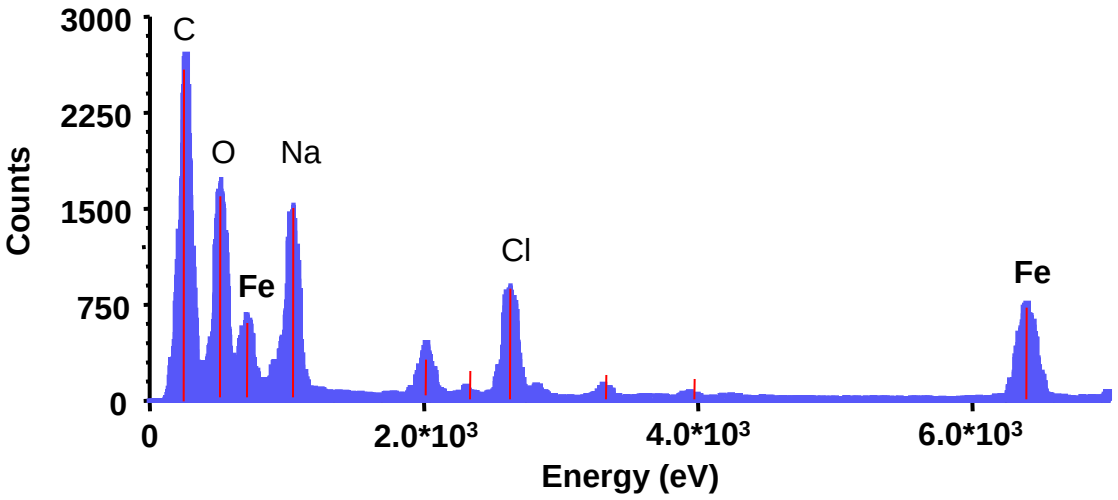
Counts
Energy (eV)
C
O
Na
Fe
Cl
Fe
3000
2250
1500
750
0
0
2.0*10³
4.0*10³
6.0*10³

(d)

(i)

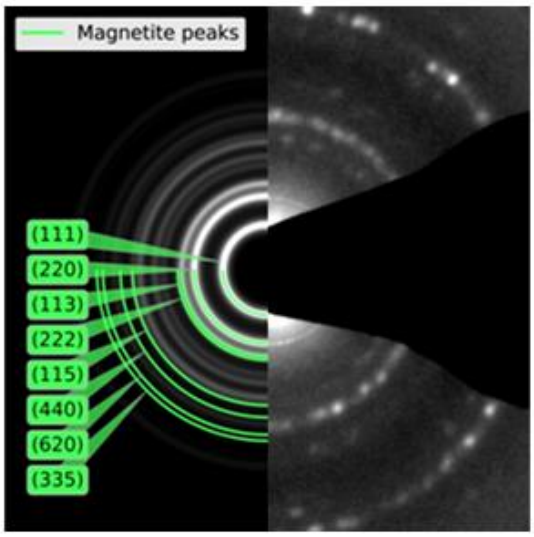
Magnetite peaks
(111)
(220)
(113)
(222)
(115)
(440)
(620)
(335)

(ii)

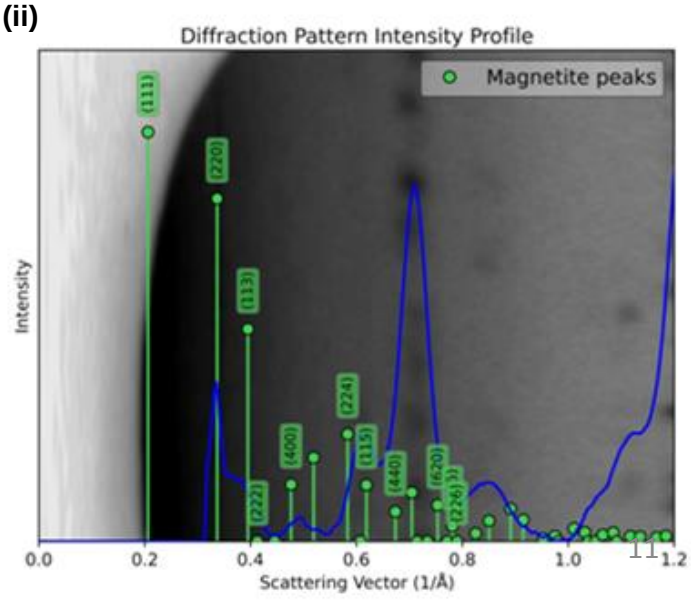
Diffraction Pattern Intensity Profile
Magnetite peaks
Intensity
Scattering Vector (1/Å)
(111)
(220)
(113)
(222)
(400)
(224)
(115)
(440)
(620)
(335)
0.0
0.2
0.4
0.6
0.8
1.0
1.2

FIGURE S1: Physical characterization of siPLK1-StAv-SPIONs. (a) TEM image of SPION core (scale bar = 20nm). (b) Frequency distribution chart showing mean diameter of SPION core is 10nm. (c) Diagram illustrating the Energy dispersive X-ray spectroscopy spectra for Iron oxide characterization peaks. (d) SAED patterns for siPLK1-StAv-SPIONs, redrawn using diffraction ring profiler. (i) SAED pattern shows polycrystalline pattern, line numbers assigned as per standard crystal lattice peaks (hkl). (ii) SAED single crystal diffraction pattern spots of the siPLK1-StAv-SPIONs are labeled with crystallographic planes of magnetite based on the measured d spacings. Green spectral lines illustrates standard magnetite diffraction pattern whereas blue illustrates siPLK1-StAv-SPIONs crystal diffraction pattern spots.

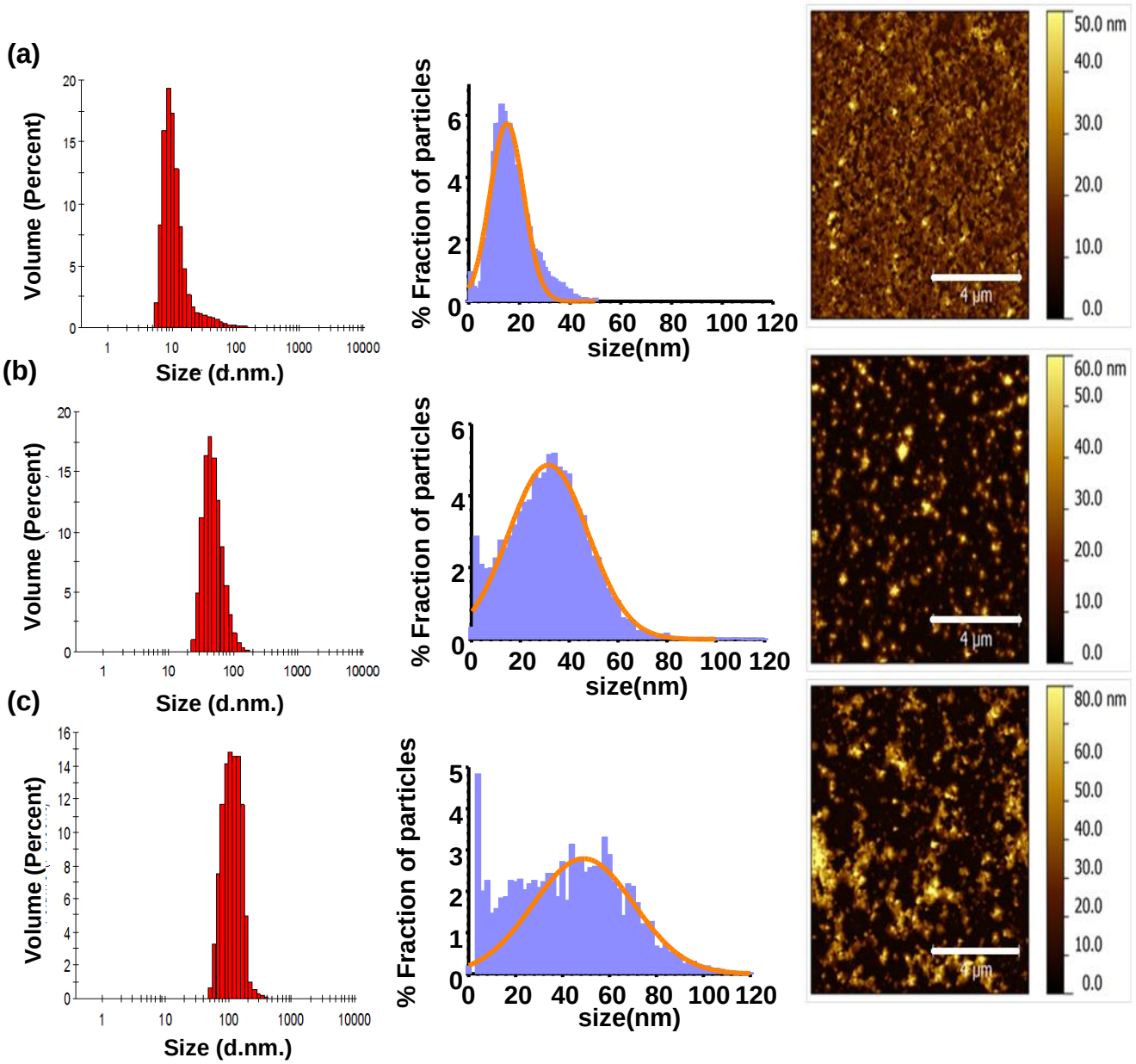

FIGURE S2: Physical characterization of siPLK1-StAv-SPIONs. Diagram shows Differential Light Scattering (DLS) graphs and Atomic Force Microscopy (AFM) images of (A) SPIONs, (B) StAv-SPIONs and (C) siPLK1-StAv-SPIONs. Bar diagrams represent the size distribution of respective group. AFM imaging reveals the surface modification of SPIONs after binding of streptavidin (StAv-SPIONs) and subsequent binding of siPLK1, MPAP- and EPPT1 (siPLK1-StAv-SPIONs).

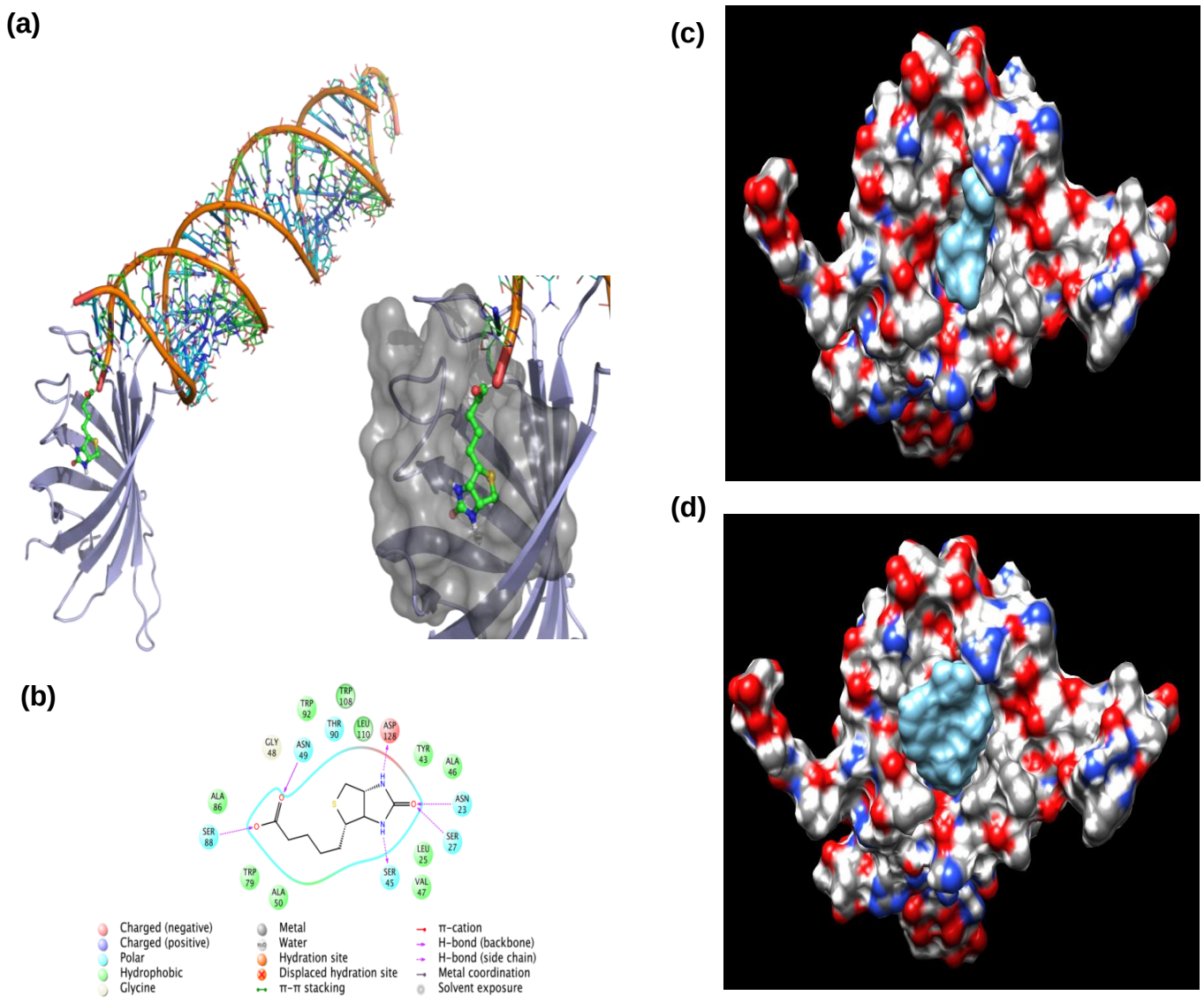

FIGURE S3: In-silico modeling of siPLK1 binding to StAv. (a) In-silico modeling of conjugation of biotinylated siRNA (Green Biotin) with StAv (gray ribbons) revealed the binding of siRNA is always above the surface of StAv and not interacting with StAv coating. Diagram in insert shows biotin binding to biotin binding pockets of StAv. (b) In-silico docking illustrating biotin binding in biotin binding pockets of StAv. (c) In-silico docking of Biotin with StAv at relative free binding energy as -18.03 kcal/mol. Biotin (in blue) depicts binding to StAv. (d) In-silico docking of biotinylated-siRNA with StAv at relative free binding energy as -11.89 kcal/mol. Biotinylated siRNA (in blue) depicts binding to StAv. with no interaction of siRNA with StAv.

FIGURE S4: Representative images of control cells, StAv-SPIONs treated cells, siControl-StAv-SPIONs and siPLK1-StAv-SPIONs 2 hours after treatment. siControl-StAv-SPIONs and siPLK1-StAv-SPIONs showed pronounced uptake of probes inside the cells as evident by brown pellets.

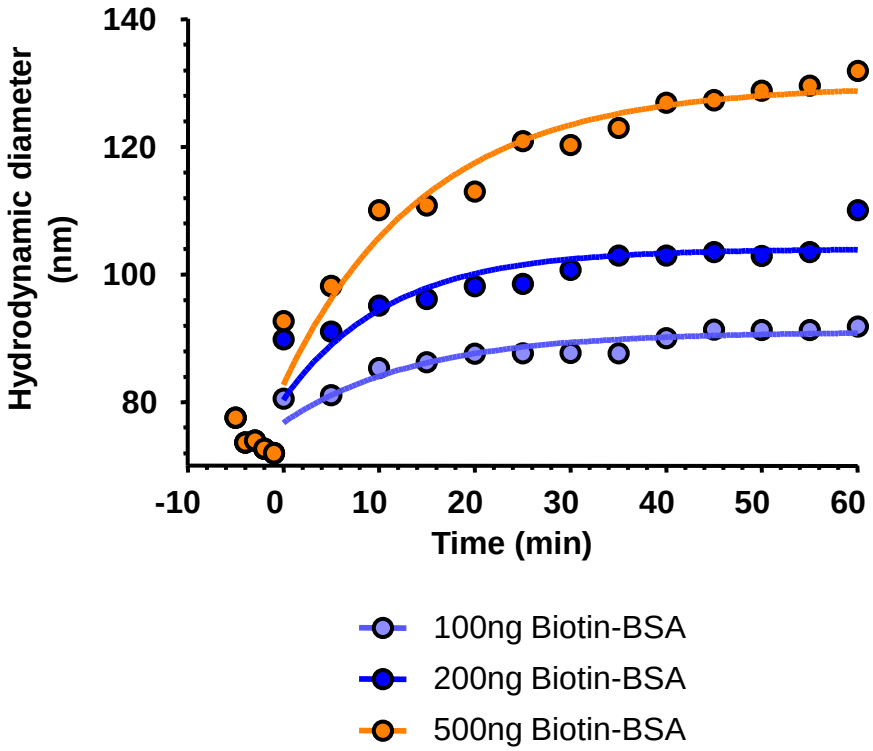

FIGURE S5: Diagram showing binding efficiency of streptavidin on coupling with SPIONs. Time dependent change in hydrodynamic diameter (d.nm) on incubation of different concentrations of biotylated BSA over the period of 60 minutes. Higher concentrations of biotinylated-BSA showed time dependent increment in hydrodynamic diameter of particles revealing binding of streptavidin to SPIONs.

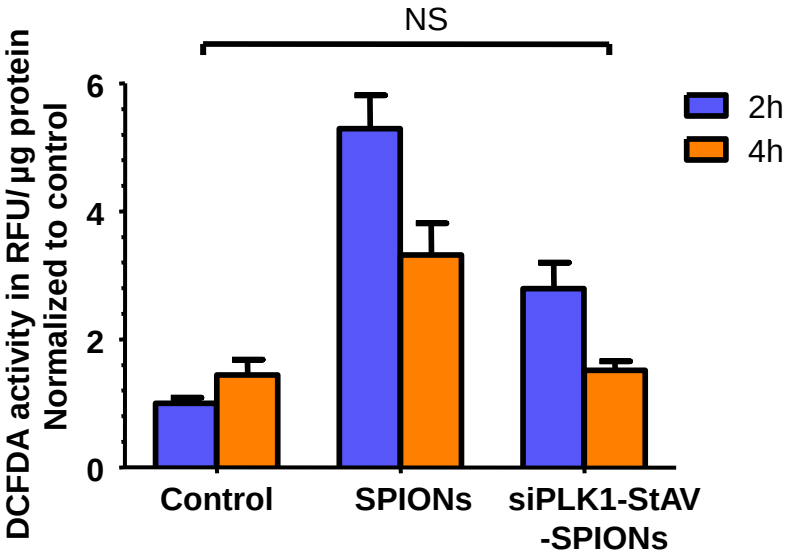

FIGURE S6: *In vitro* tolerance on generation in reactive oxygen species on treatment of siPLK1-StAv-SPIONs to the tumors. DC-FDA fluorescence was evaluated after 2 and 4 hours of treatment of SPIONs and siPLK1-StAv-SPIONs showed better tolerance than siPLK1-StAv-SPIONs. Data was expressed as mean ± SD (n=3).

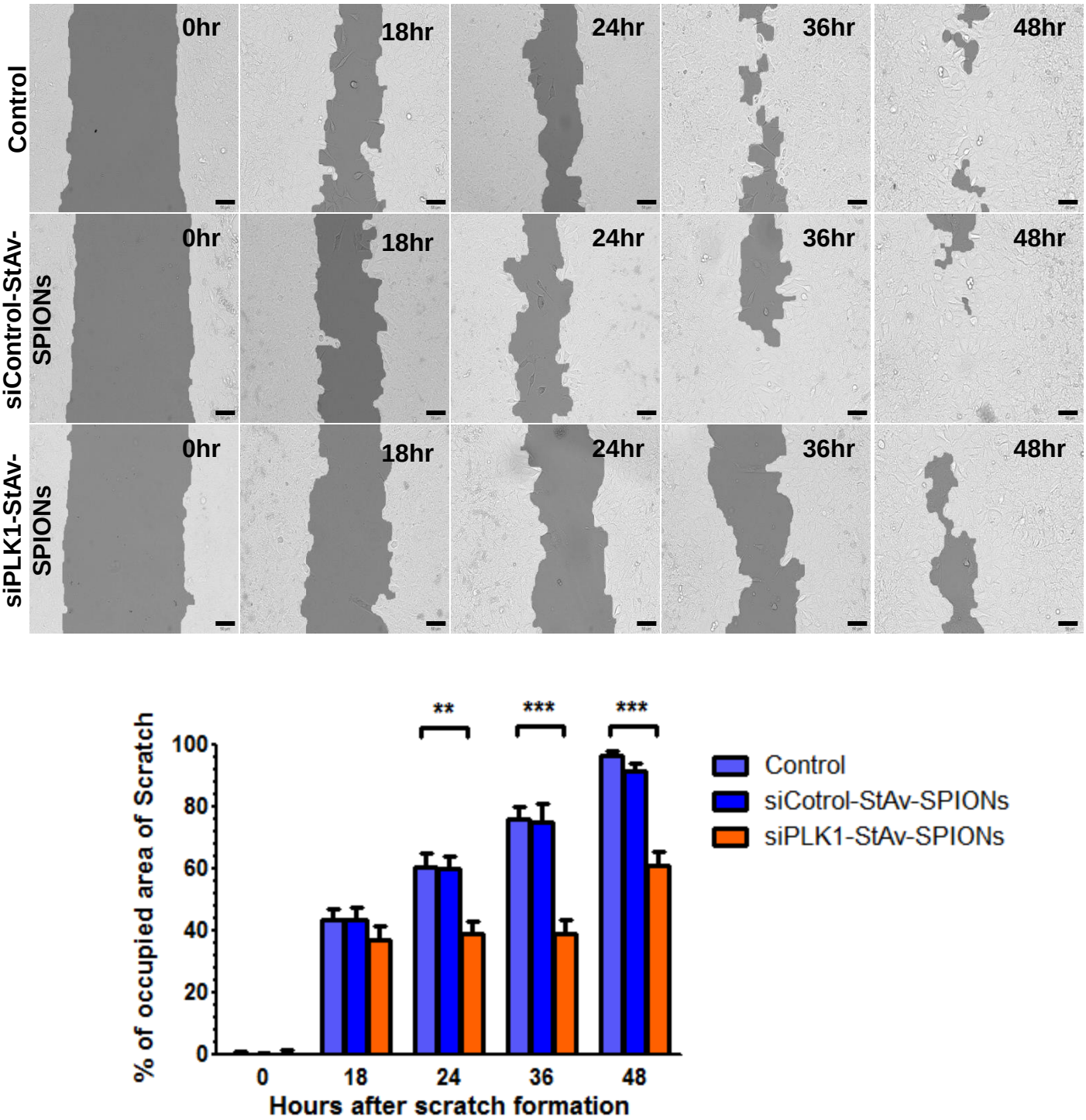

FIGURE S7: *In-vitro* migratory potentials of tumour cells on siPLK1-StAv-SPIONs treatment was manifested by scratch assay over a period of 48 hours. siPLK1-StAv-SPIONs treatment showed decrease in migratory potential of cancer cells compared to that of corresponding controls.

(a)

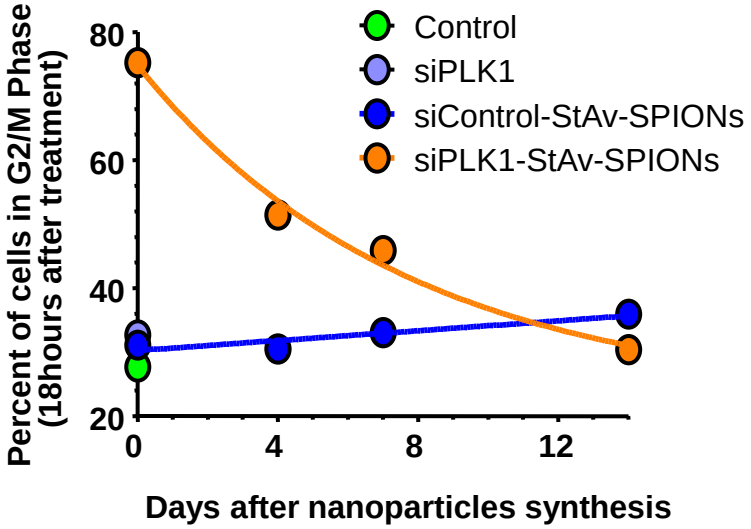

(b)

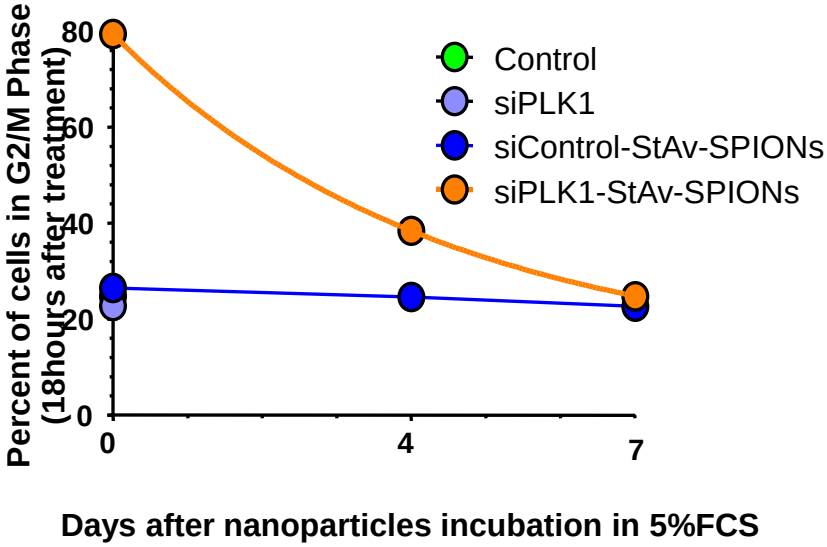

FIGURE S8: In solution stability of siPLK1-StAv-SPIONs. (a) siPLK1-StAv-SPIONs were incubated in saline at 37^0C for 0, 4, 7 and 14 days. The influence of siPLK1-StAv-SPIONs on stabilizing G2/M phase of cell cycle was evaluated. (b) siPLK1-StAv-SPIONs were incubated in 5% FCS at 37^0C for 0, 4, and 7 days. The influence of siPLK1-StAv-SPIONs on stabilizing G2/M phase of cell cycle was evaluated. It was observed that siPLK1-StAv-SPIONs are stable in solution for around 4 days.

(a)

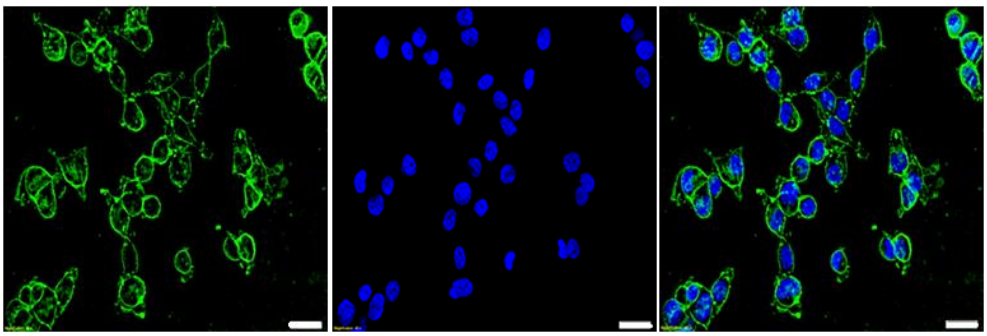
MUC1
DAPI
MUC1/DAPI

(b)

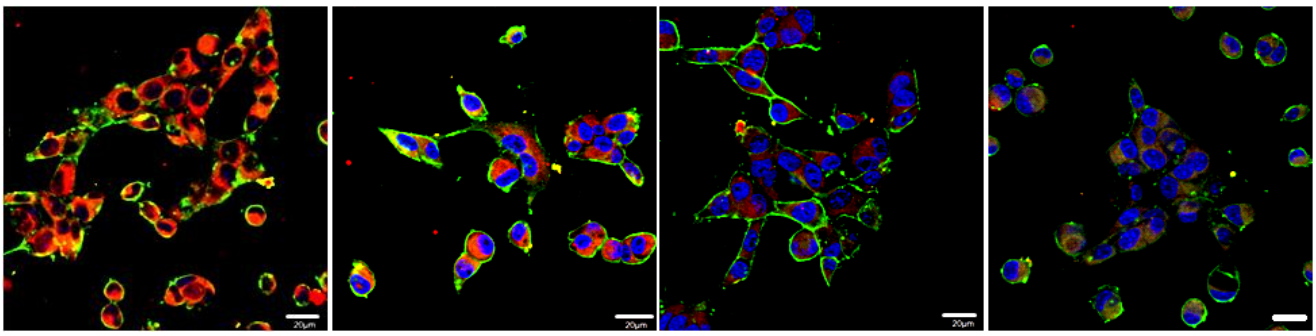
Cy5-siPLK1-StAv-SPIONs/Oregon Green 488/DAPI
Control,0μg/ml
Anti-MUC1,0.5μg/ml
Anti-MUC1,1μg/ml
Anti-MUC1,2.5μg/ml

(c)

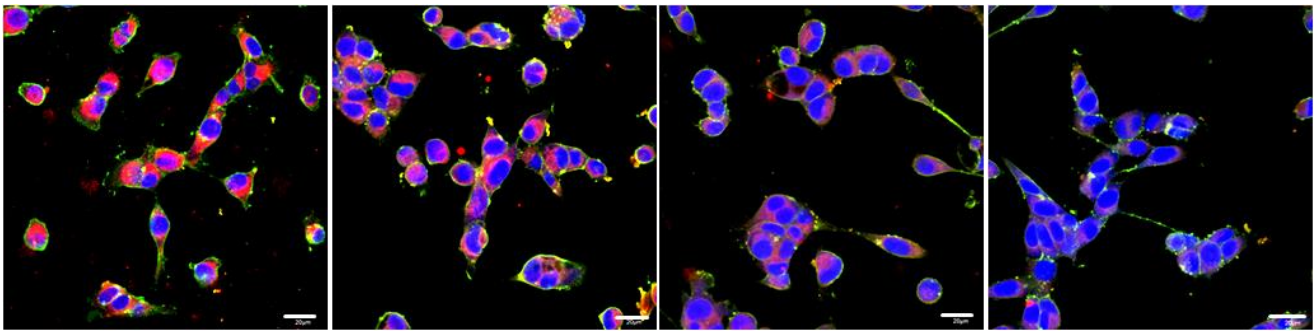
Cy5-siPLK1-StAv-SPIONs/Oregon Green 488/DAPI
Control,0μM
Dynasore,10μM
Dynasore,20μM
Dynasore,50μM

(d)

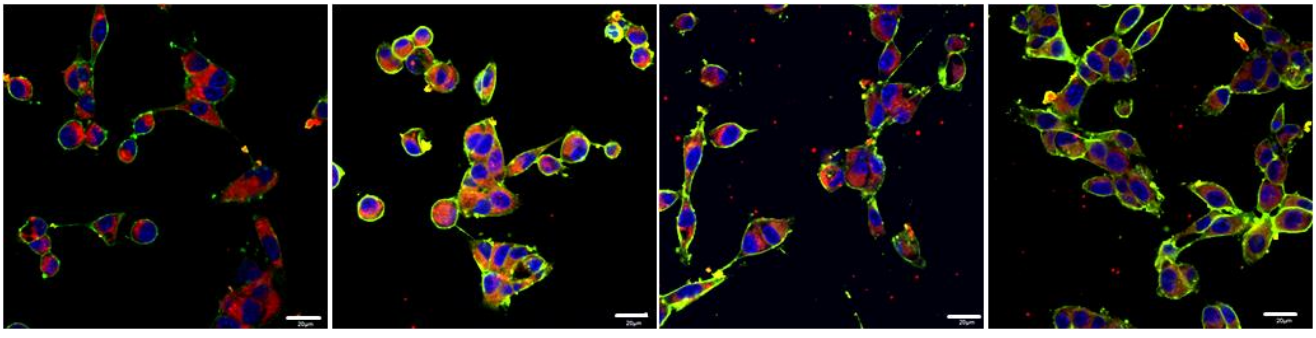
Cy5-siPLK1-StAv-SPIONs/Oregon Green 488/DAPI
Control,0μM
MDC,10μM
MDC,50μM
MDC,100μM

FIGURE S9: Fluorescence imaging on treatment of anti-MUC1 antibody, Dynasore and MDC to evaluate uptake mechanism. siPLK1-StAv-SPIONs were further conjugated with biotinylated Cy5(red) to analyze particles using fluorescence microscopy. Plasma membrane was stained in Oregon green (green) and nuclei in blue. (a) Immunofluorescence staining of MUC1 showing surface localization of MUC1 on pancreatic cancer cell-line, 6606PDA. (b) Blockage of MUC1 by Anti-MUC1 antibody showed a concentration dependent reduction in the uptake of siPLK1-StAv-SPIONs. (c) Dynasore, an inhibitor of clathrin dependent endocytosis through inhibition of Dynamin and therefore preventing uncoating, showed a concentration dependent decrease in the uptake of siPLK1-StAv-SPIONs. (d) Monodansylcadaverine (MDC) believed to inhibit clathrin mediated endocytosis by stabilizing nascent clathrin-coated pits confirmed a time dependent reduction in uptake of siPLK1-StAv-SPIONs upon inhibition of clathrin mediated endocytosis.

(a)

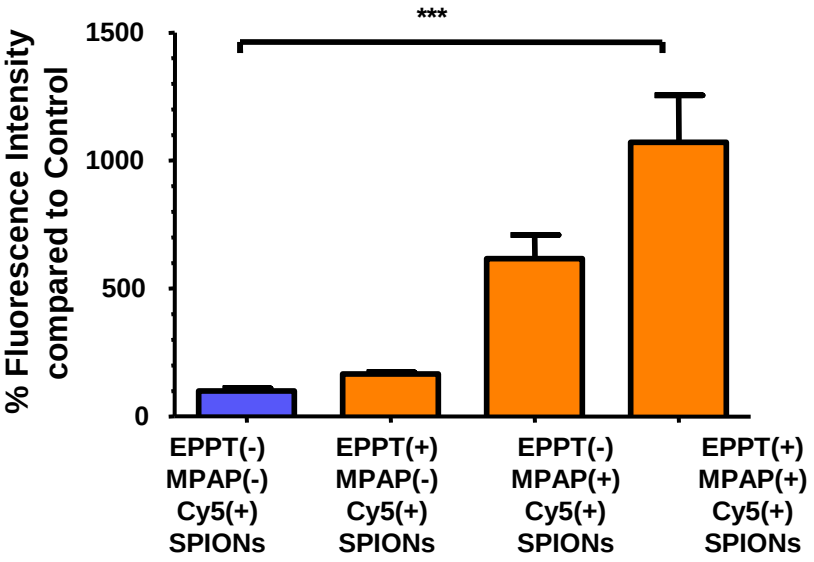
***
1500
1000
500
0
% Fluorescence Intensity compared to Control
EPPT(-) MPAP(-) Cy5(+) SPIONs
EPPT(+) MPAP(-) Cy5(+) SPIONs
EPPT(-) MPAP(+) Cy5(+) SPIONs
EPPT(+) MPAP(+) Cy5(+) SPIONs

(b)

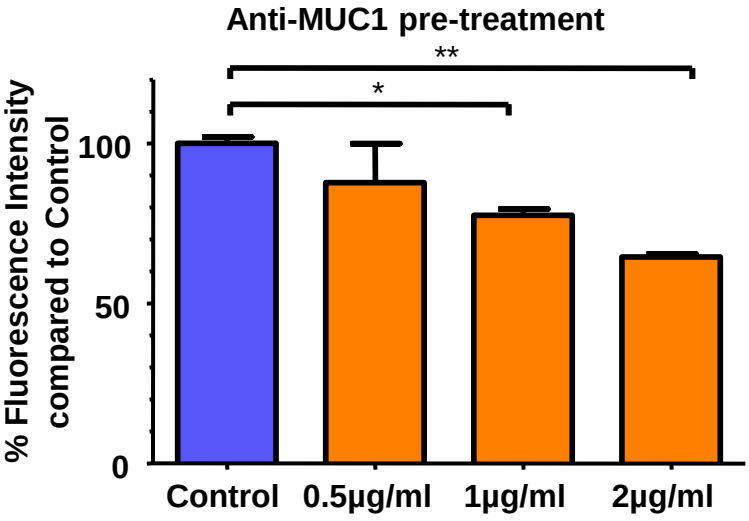
Anti-MUC1 pre-treatment
**
*
100
50
0
% Fluorescence Intensity compared to Control
Control
0.5µg/ml
1µg/ml
2µg/ml

(c)

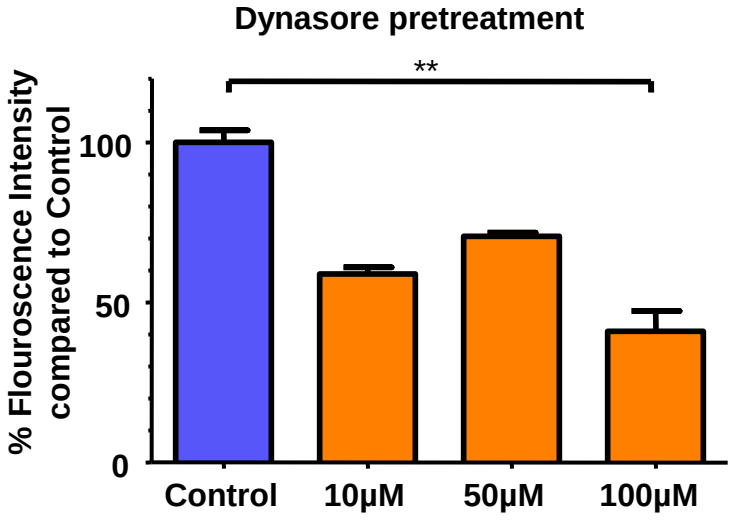
Dynasore pretreatment
**
100
50
0
% Flouroscence Intensity compared to Control
Control
10µM
50µM
100µM

FIGURE S10: *In-vitro* uptake analysis of siPLK1-StAv-SPIONs using fluorescence associated cell sorting. Upon treatment with Cy 5 (red) conjugated siPLK1-StAv-SPIONs, cells were fixed, permeabilized and evaluated for Cy5 (red) positive cells marking siPLK1-StAv-SPIONs. (a) Quantitative analysis showed the percentage of uptake of siPLK1-StAv-SPIONss with EPPT1 and MPAP (MPAP(+)EPPT1(+)SPIONs) in 6606PDA. siPLK1-StAv-SPIONs without EPPT1 and MPAP (MPAP(-)EPPT1(-)SPIONs) were taken up to a lesser extent. (b) Quantitative analysis showed a decrease in uptake of siPLK1-StAv-SPIONs after anti-MUC1 treatment. (c) Quantitative analysis showed reduced uptake of siPLK1-StAv-SPIONs after Dynasore treatment. Data are expressed as mean ± SD from 3 individual experiments. ***$p<0.001$, **$p<0.01$, *$p<0.05$ considered statistically significant.

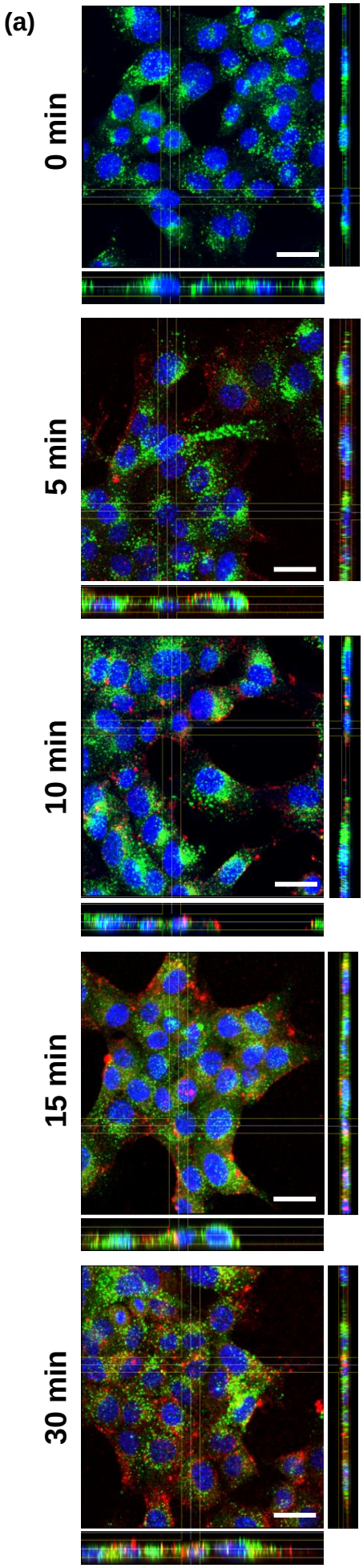

FIGURE S11: Co-localization of siPLK1-StAv-SPIONs with endosomes. Treatment of Cy5 conjugated siPLK1-StAv-SPIONs for 0, 5, 10, 15 and 30 min showed co-localization of Cy5 conjugated siPLK1-StAv-SPIONs with EEA-1, an endosomal marker as early as 5 min. (a) Representative images showed co-localization at different time points. (b) Pearson co-localization coefficient, depicting approx. 20% Cy5 conjugated siPLK1-StAv-SPIONs co-localized with EEA1 at a given time point as shown in the bar diagram. Data expressed as mean ± SD from 4 individual experiments. **p<0.01, *p<0.05 considered statistically significant .

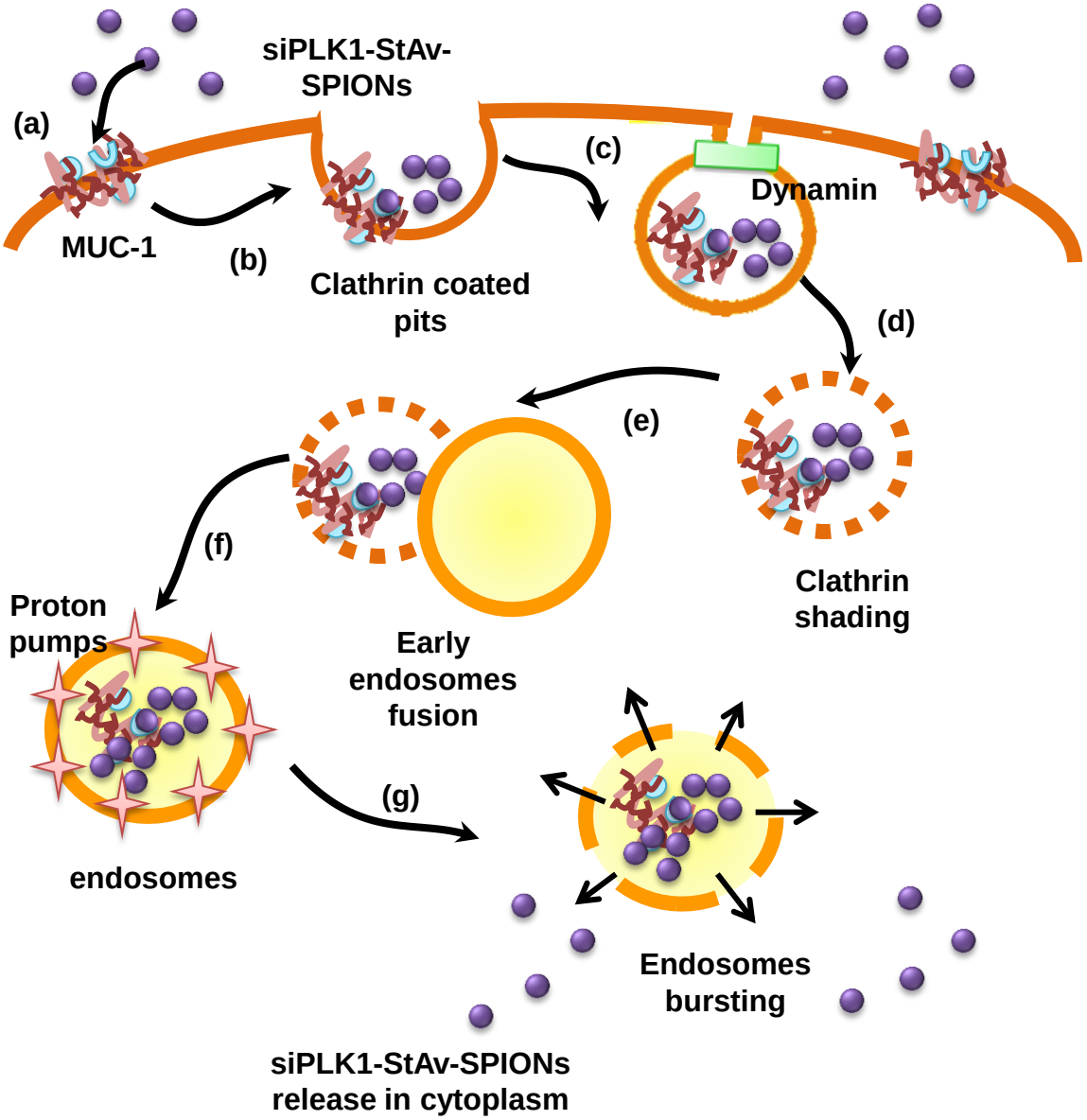

FIGURE S12: Possible uptake and release mechanism of siPLK1-StAv-SPIONs. (a) siPLK1-StAv-SPIONs bind selectively to MUC1 expressing cells through the aid of EPPT1 and MPAP. (b) The cells start forming clathrin coated pits along the siPLK1-StAv-SPIONs. (c) These pits undergo scission, which is mediated by Dynamin. (d) The formed vesicles get internalized, where clathrin is shaded. (e-f) Clathrin shaded vesicles fuse with early endosomes to form endosomes. (g) Inside endosomes unsaturated amino acid groups from MPAP sequester protons through proton pumps. This builds an osmotic pressure inside the endosomes resulting in the membrane rapture of endosomes and the release of siPLK1-StAv-SPIONs into the cytoplasm. Here the siRNA can work vis the RISC complex.

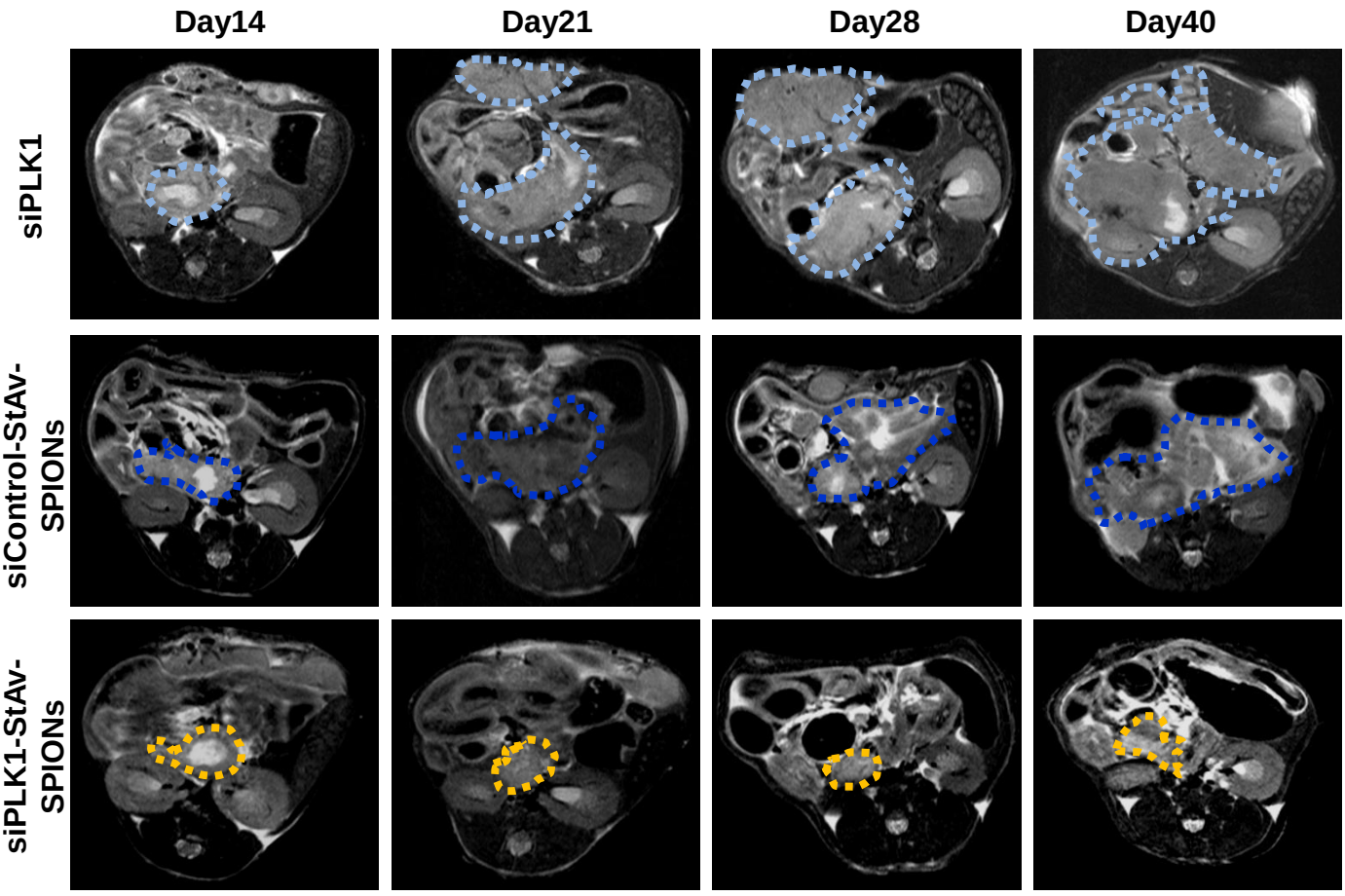

FIGURE S13: *In situ* measurement of tumor volume using MRI. Mice bearing a syngenic orthotopic tumor were imaged for tumor volume measurement at 14, 21, 28 and 40 days after siPLK1, siControl-StAv-SPIONs and siPLK1-StAv-SPIONs treatment (twice a week for four weeks) starting at day 14 after tumor implantation. Figures show representative image per time point.

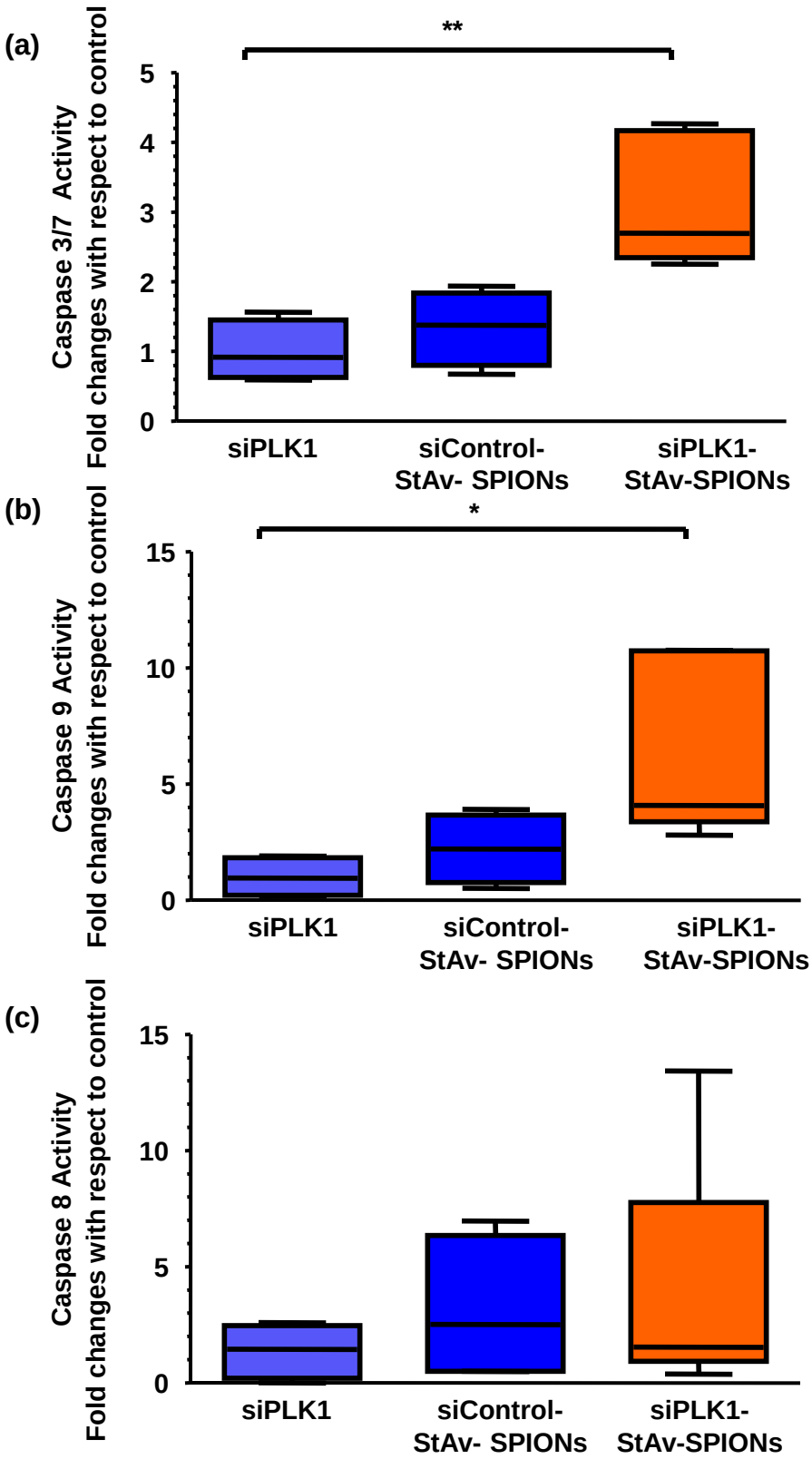

FIGURE S14: Influence of siPLK1-StAv-SPIONs treatment on caspases activity cascade. Caspase 3/7 (a), caspase 9 (b) and caspase 8 (c) activity in tumor tissues of syngenic orthotopic tumour model of different treatment groups was measured using the flourogenic substrates R110-DEVD (caspase 3/7), AMC-IETD (caspase 8) and R110-LETD (caspase 9) (n=4-5 animals). **p<0.01, *p<0.05 considered statistically significant.

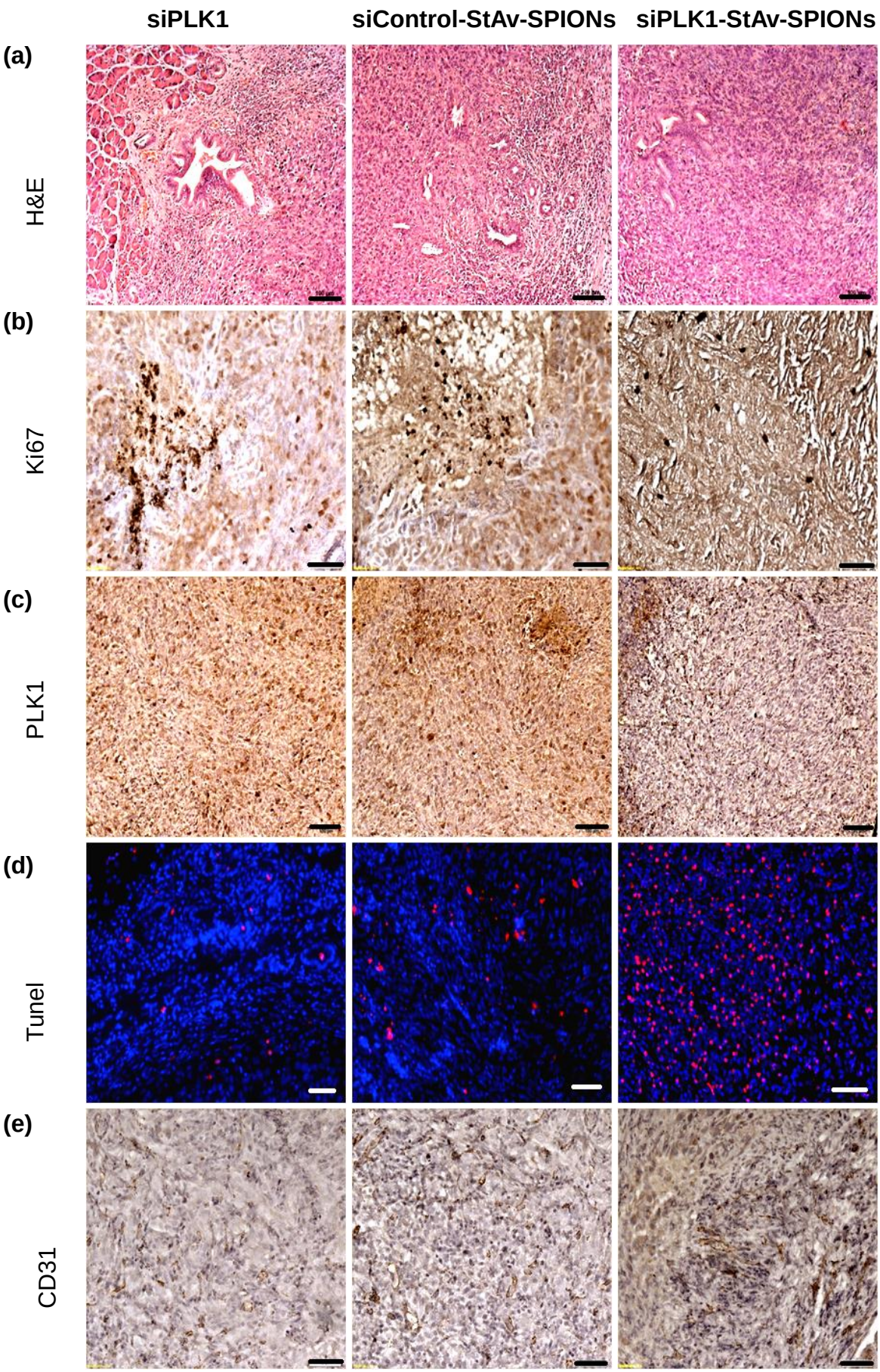
siPLK1
siControl-StAv-SPIONs
siPLK1-StAv-SPIONs
(a)
H&E
(b)
Ki67
(c)
PLK1
(d)
Tunel
(e)
CD31

FIGURE S15: Histological examination after 4 weeks treatment with siPLK1-StAv-SPIONs in mice bearing a syngenic orthotopic tumor. (a) representative images for H&E, (b) Ki67, (c) PLK1, (d) Tunel positive cells and (e) CD31. (Scale bar=100μm) siPLK1-StAv-SPIONs did not show any change in tumor angiogenesis.

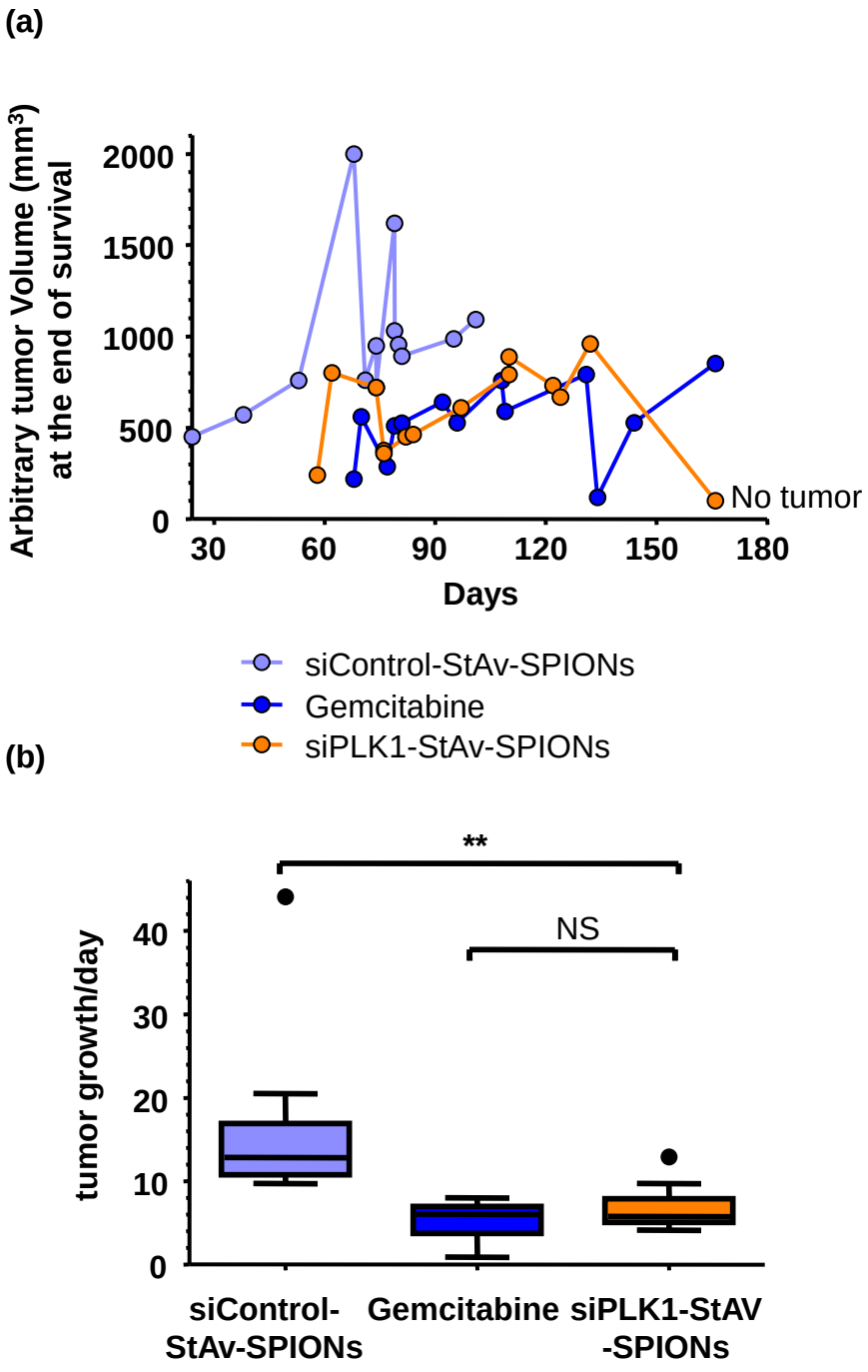

FIGURE S16: Diagram illustrating the influence of siPLK1-StAv-SPION treatment. (a) siPLK1-StAv-SPIONs showed lesser tumor burden and increased survival compared to siControl-StAv-SPIONs treatment. (b) siPLK1-StAv-SPIONs showed a delayed tumor growth per day compared to siControl-StAv-SPIONs treatment. ** $p<0.01$ considered statistically significant (n=13-14).

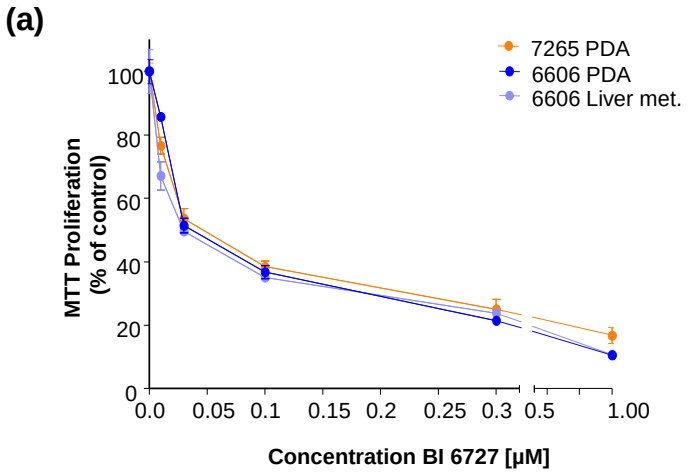

(b)

Cell line	IC_{50} BI 6727 (µM)
6606 PDA	0,09
6606 Liver	0,065
7265 PDA	0,08

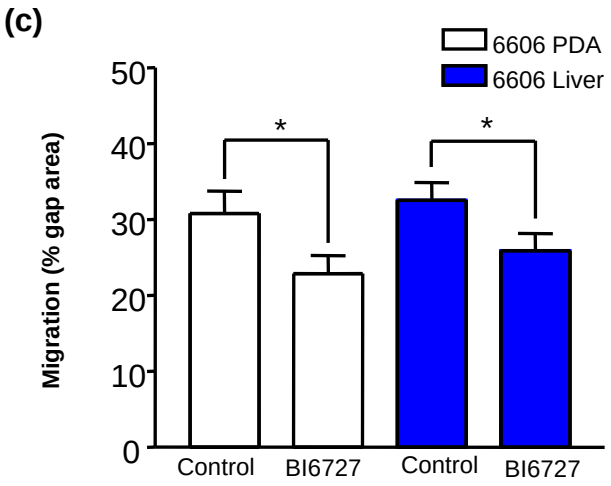

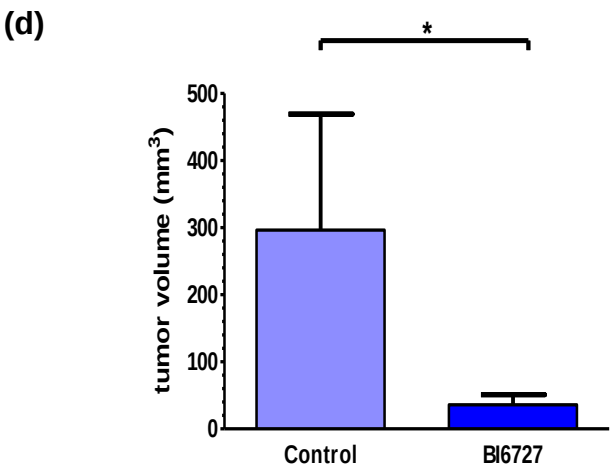

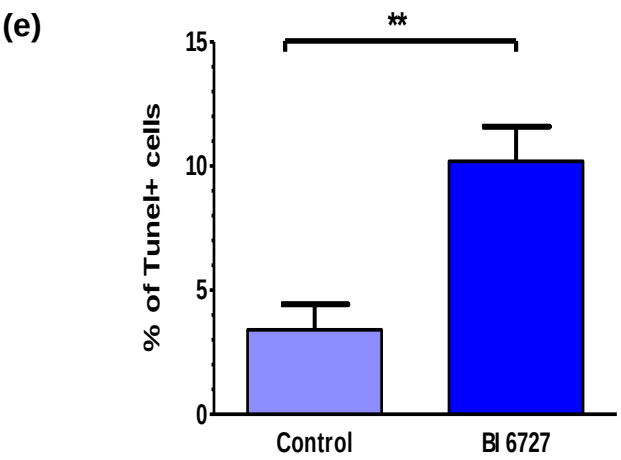

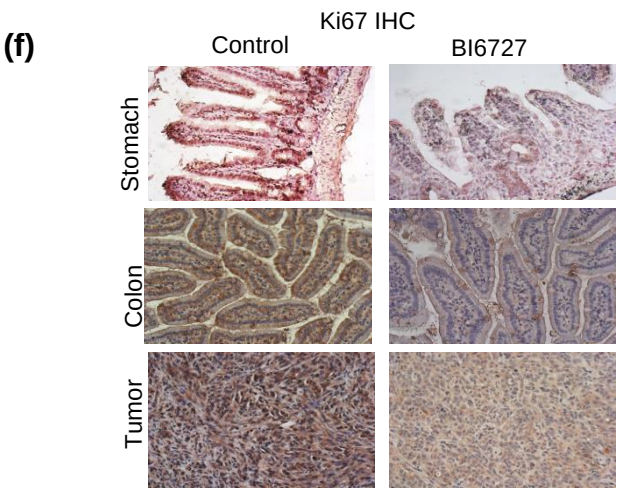

<u>Figure S17</u>: Influence of BI6727 treatment in syngenic orthotopic tumor model. Animals were treated with 25mg/kg/week BI6727 for 2 weeks and tumor were harvested at the end of treatment. **(A-B)** IC_{50} value of BI6727 in different murine pancreatic cancer cell-lines 24 hours after incubation. **(C)** Migration assay showing decrease in cell migration 24 hours after 0.1 µM BI6727 incubation. **(D**) BI6727 showed significant decrease in tumor volume. **(E)** Decrease in tumor was accompanied by increase in apoptosis as evident by increase in Tunel+ cells. **(F)** Though highly efficious in reducing tumor proliferation, BI6727, showed necrosis of stomach and colon mucosa as evident by decrease in proliferation by proliferation marker, Ki67.

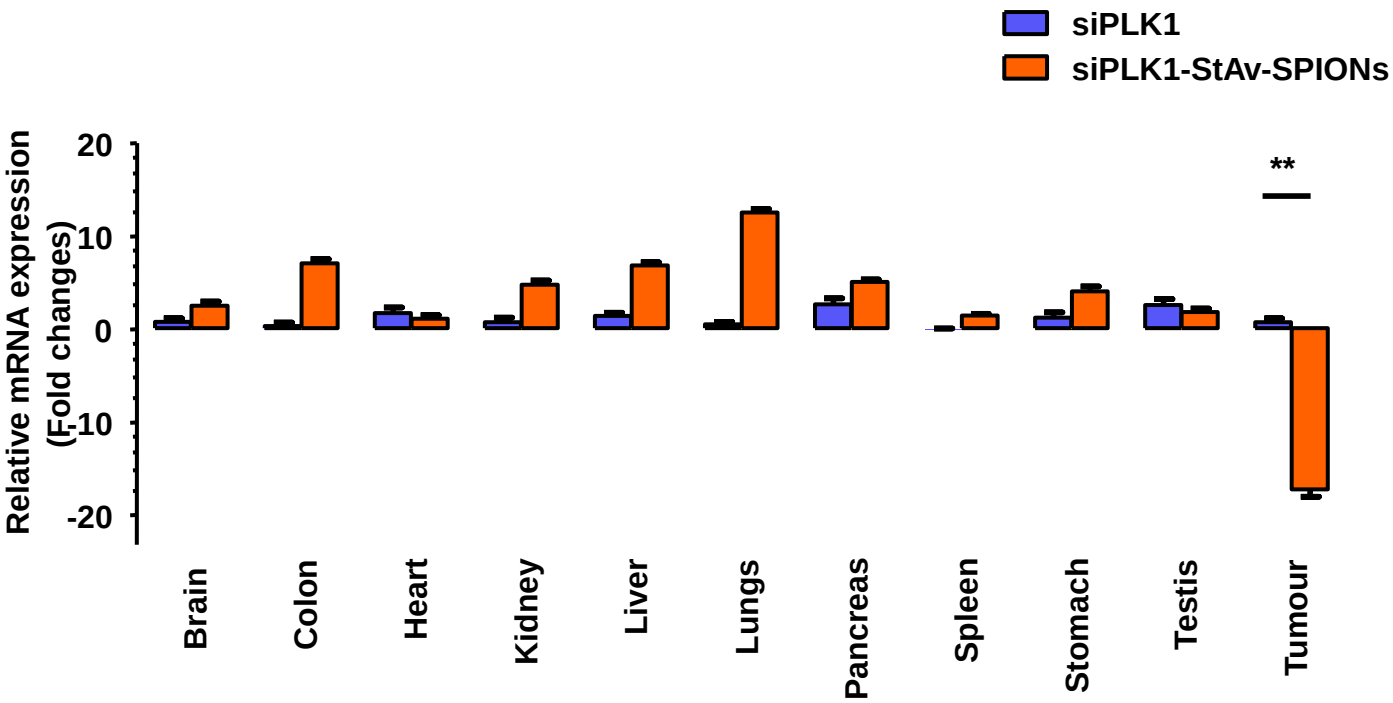

FIGURE S18: Differential expression of PLK1 upon siPLK1-StAv-SPIONs treatment. Total mRNA was isolated from different organs after siPLK1 and siPLK1-StAv-SPIONs treatment. plk1 mRNA expression levels were quantified by reverse transcription-polymerase chain reaction. Data are expressed as fold changes with respect to control in mean ± SEM (n=3). These data confirm the selective delivery *in vivo* of siPLK1-StAv-SPIONs to the tumor upon treatment with siPLK1-StAv-SPIONs. The variation in PLK1 in off-target organs is due to rapidly proliferating cells such as leukocytes which have homogenized together with the organs.

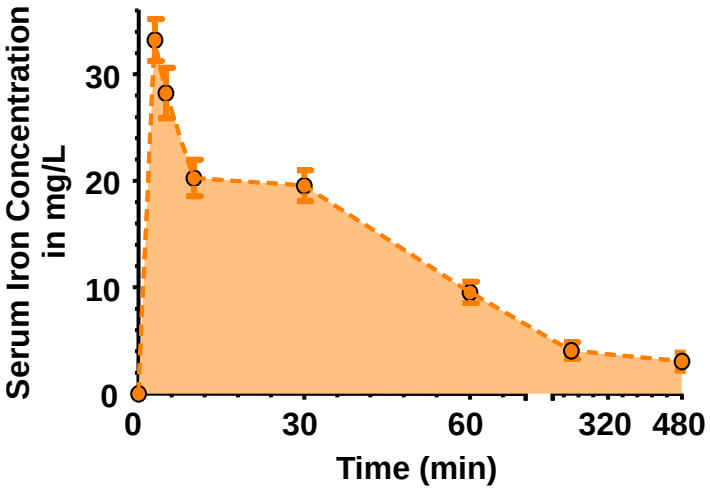

FIGURE S19: Time dependent change in serum iron concentration after single dose of siPLK1-StAv-SPIONs.

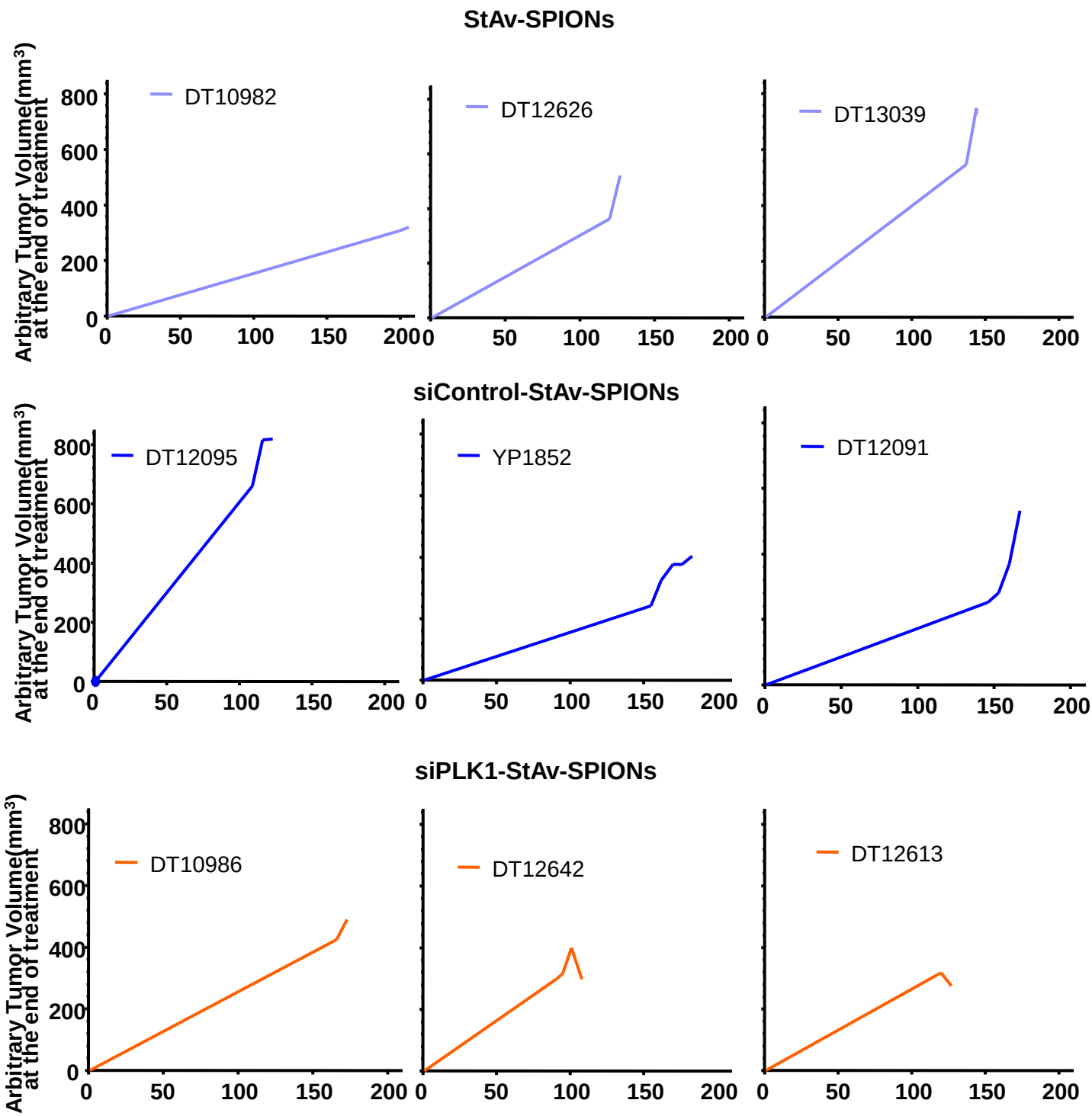

FIGURE S20: Spider diagram showing tumour growth in individual mice treated with StAv-SPIONs (light Blue), siControl-StAv-SPIONs (Deep Blue) and siPLK1-StAv-SPIONs (Orange). siPLK1-StAv-SPIONs treatment showed hindered tumor growth.

(a)

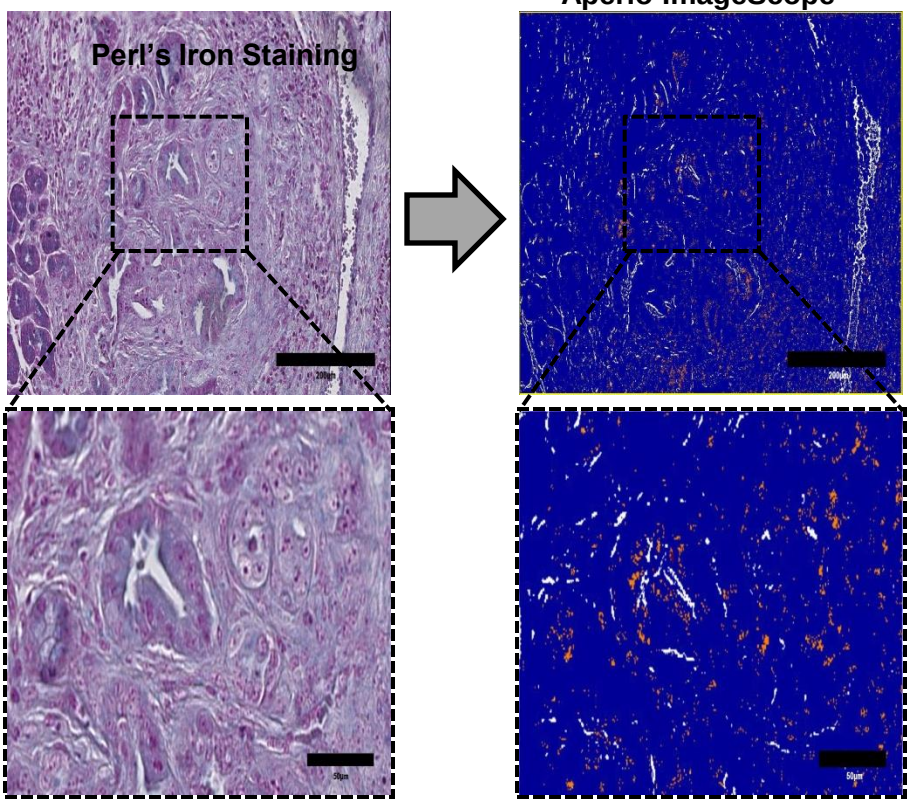
Perl's Iron Staining
Iron Quantification using
Aperio ImageScope
Positive cell count v9 algorithm
Hue value 0.66
Hue width 0.01
Saturation 0.08
Negative
Weak positive
Positive
Strong positive

(b)

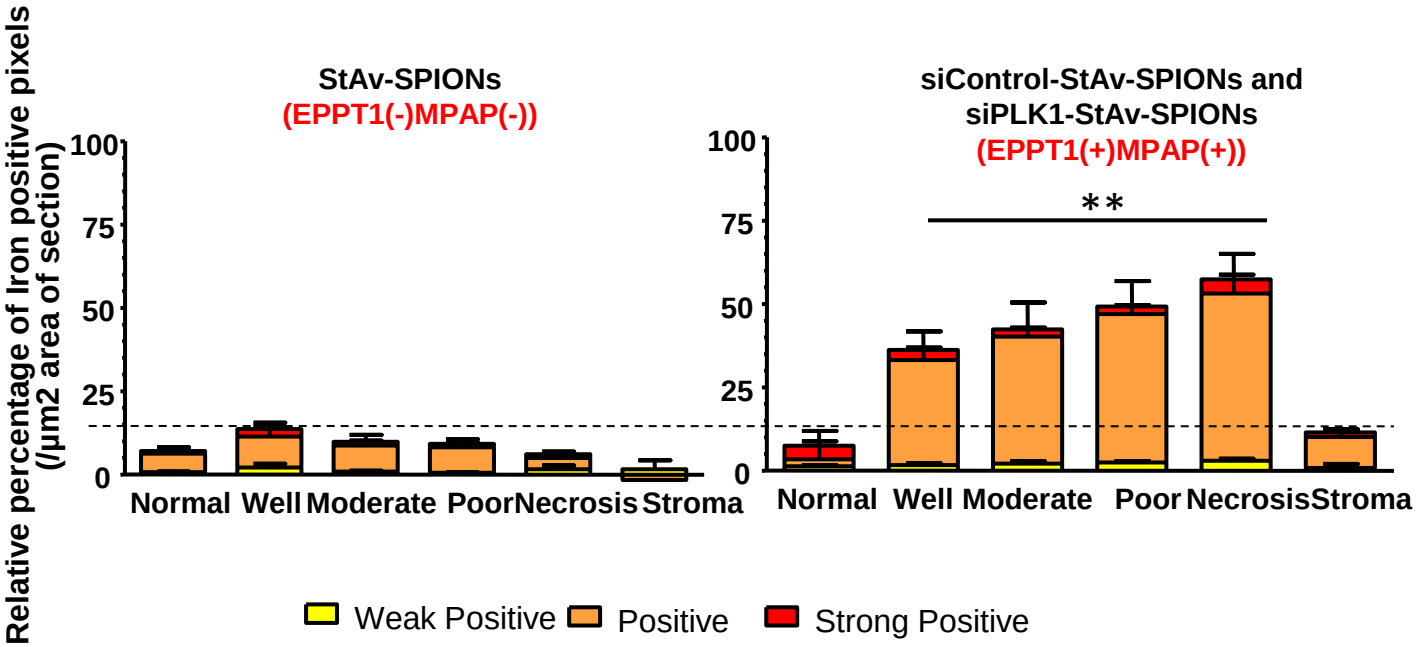
StAv-SPIONs
(EPPT1(-)MPAP(-))
siControl-StAv-SPIONs and
siPLK1-StAv-SPIONs
(EPPT1(+)MPAP(+))
**
Relative percentage of Iron positive pixels
(/μm2 area of section)
100
75
50
25
0
Normal
Well
Moderate
Poor
Necrosis
Stroma
Weak Positive
Positive
Strong Positive

FIGURE S21: Quantification of iron accumulation in $Kras^{G12D}p53^{R172H}$pdx.cre (KPC) mice on siPLK1-StAv-SPIONs treatment. (a) Representative images showing quantification methodology for SPIONs uptake on Perls iron staining using Apario ImageScope software. Scale bar= 200µm (Insert scale bar= 50µm). **(b)** Graphical representation illustration SPIONs uptake in well. Moderate, poor differentiated tumour cells, necrotic area, stroma and normal pancreatic cells. ** $p<0.01$ (n=4 for StAv-SPIONs, n=9 for nanoparticulate probes)

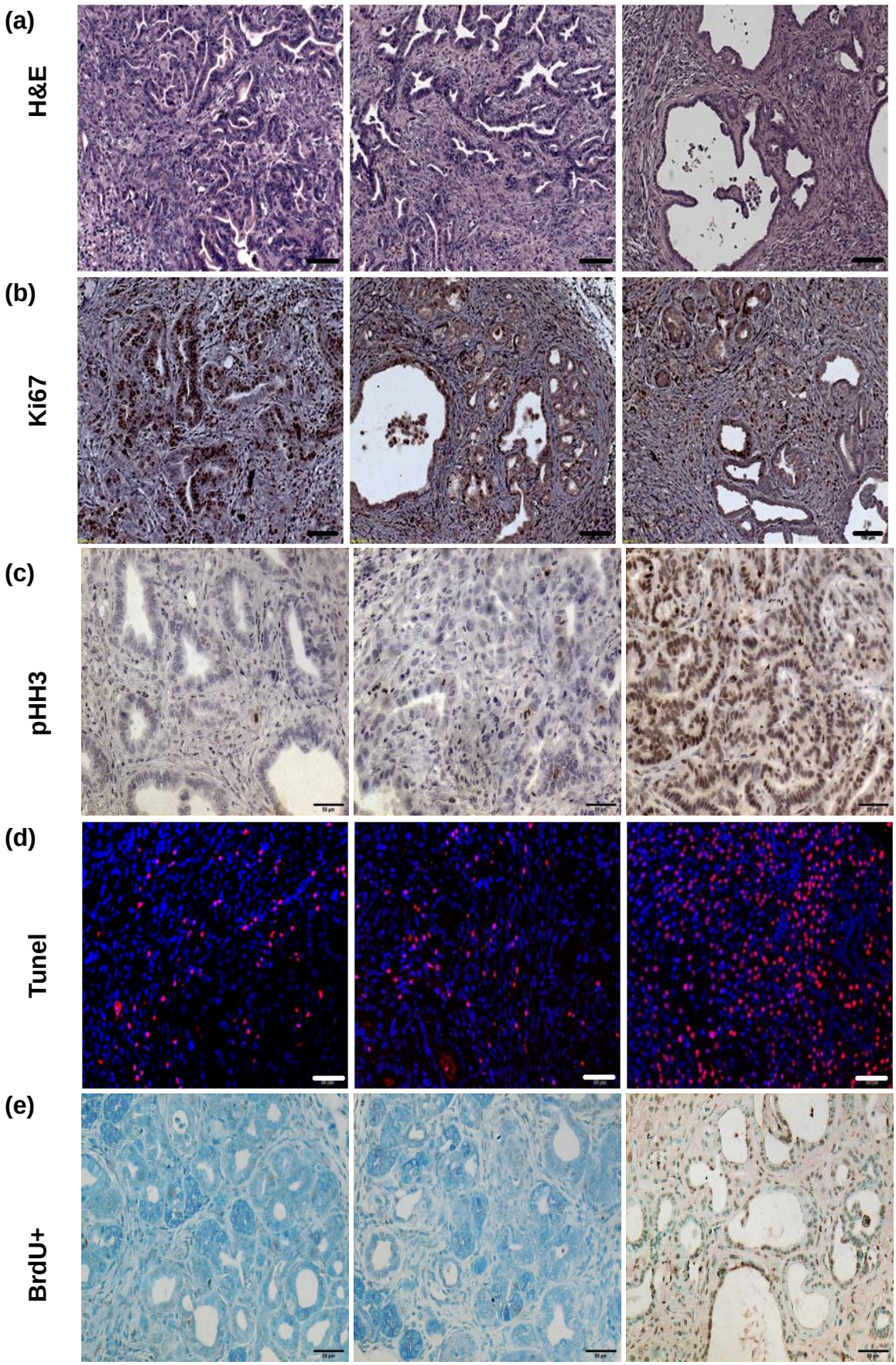
StAv-SPIONs
siControl-StAv -SPIONs
siPLK1-StAv -SPIONs
(a)
H&E
(b)
Ki67
(c)
pHH3
(d)
Tunel
(e)
BrdU+

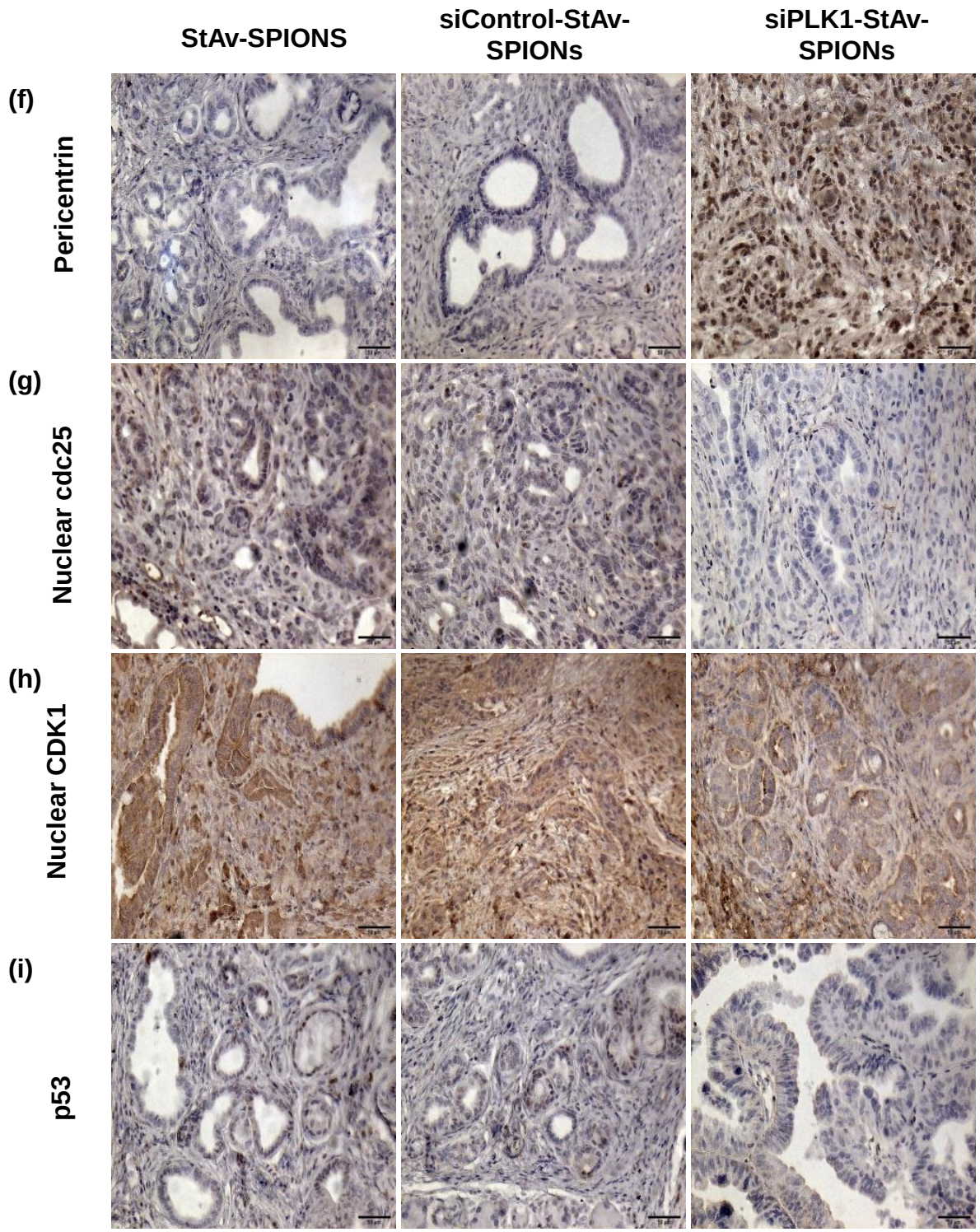

FIGURE S22: Histological examination after 2 weeks treatment of siPLK1-StAv-SPIONs in KPC mice. (a) representative images for H&E (Scale bar=100µm), (b) Ki67 (Scale bar=100µm), (c) phospho Histone H3 (Scale bar= 50µm), (d) Tunel positive cells. (Scale bar=100µm) (e) BrdU (Scale bar= 50µm), (f) Pericentrin, (Scale bar= 50µm), (g) Nuclear cdc25 (Scale bar= 50µm), (h) CDK1 (Scale bar= 50µm) and (i) p53 (Scale bar= 50µm)

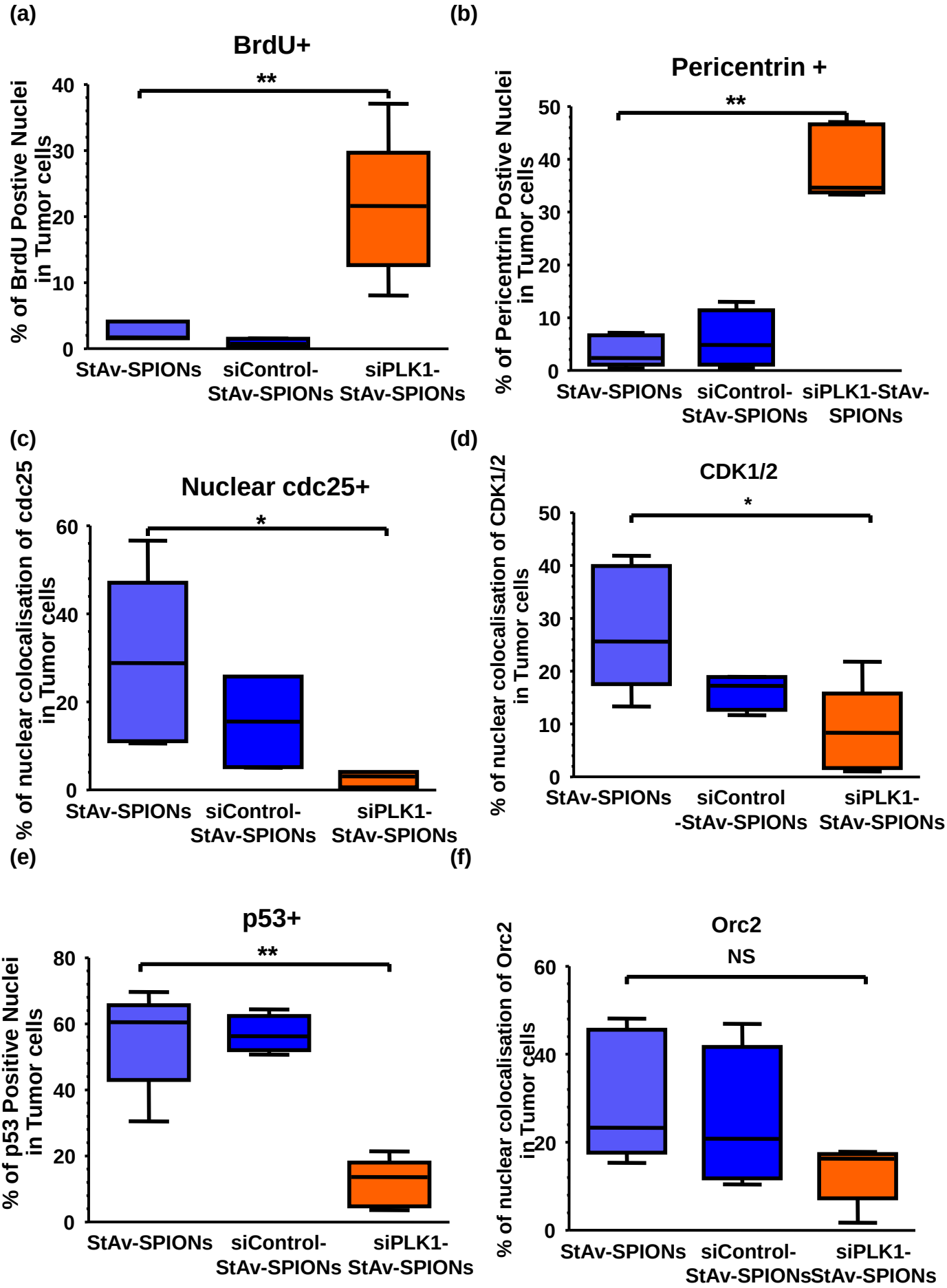
(a)
BrdU+
**
% of BrdU Postive Nuclei in Tumor cells
40
30
20
10
0
StAv-SPIONs
siControl-StAv-SPIONs
siPLK1-StAv-SPIONs
(b)
Pericentrin +
**
% of Pericentrin Postive Nuclei in Tumor cells
50
40
30
20
10
0
StAv-SPIONs
siControl-StAv-SPIONs
siPLK1-StAv-SPIONs
(c)
Nuclear cdc25+
*
% of nuclear colocalisation of cdc25 in Tumor cells
60
40
20
0
StAv-SPIONs
siControl-StAv-SPIONs
siPLK1-StAv-SPIONs
(d)
CDK1/2
*
% of nuclear colocalisation of CDK1/2 in Tumor cells
50
40
30
20
10
0
StAv-SPIONs
siControl-StAv-SPIONs
siPLK1-StAv-SPIONs
(e)
p53+
**
% of p53 Positive Nuclei in Tumor cells
80
60
40
20
0
StAv-SPIONs
siControl-StAv-SPIONs
siPLK1-StAv-SPIONs
(f)
Orc2
NS
% of nuclear colocalisation of Orc2 in Tumor cells
60
40
20
0
StAv-SPIONs
siControl-StAv-SPIONs
siPLK1-StAv-SPIONs

FIGURE S23: Change in expression of different downstream molecules, proliferation markers and apoptotic markers in KPC mice upon siPLK1-StAv-SPIONs treatment. After 2 weeks of siPLK1-StAv-SPIONs treatment, tumor showed significant increment in, BrdU positive nuclei (a), pericentrin (b), and significant reduction in nuclear cdc25 localisation (c), nuclear CDK1/2 localisation (d) and p53 (e), expression if compared to controls. ** $p<0.01$, * $p<0.05$ (n=4-5). Orc2 (f) did not show any statistically significant deviation in expression.

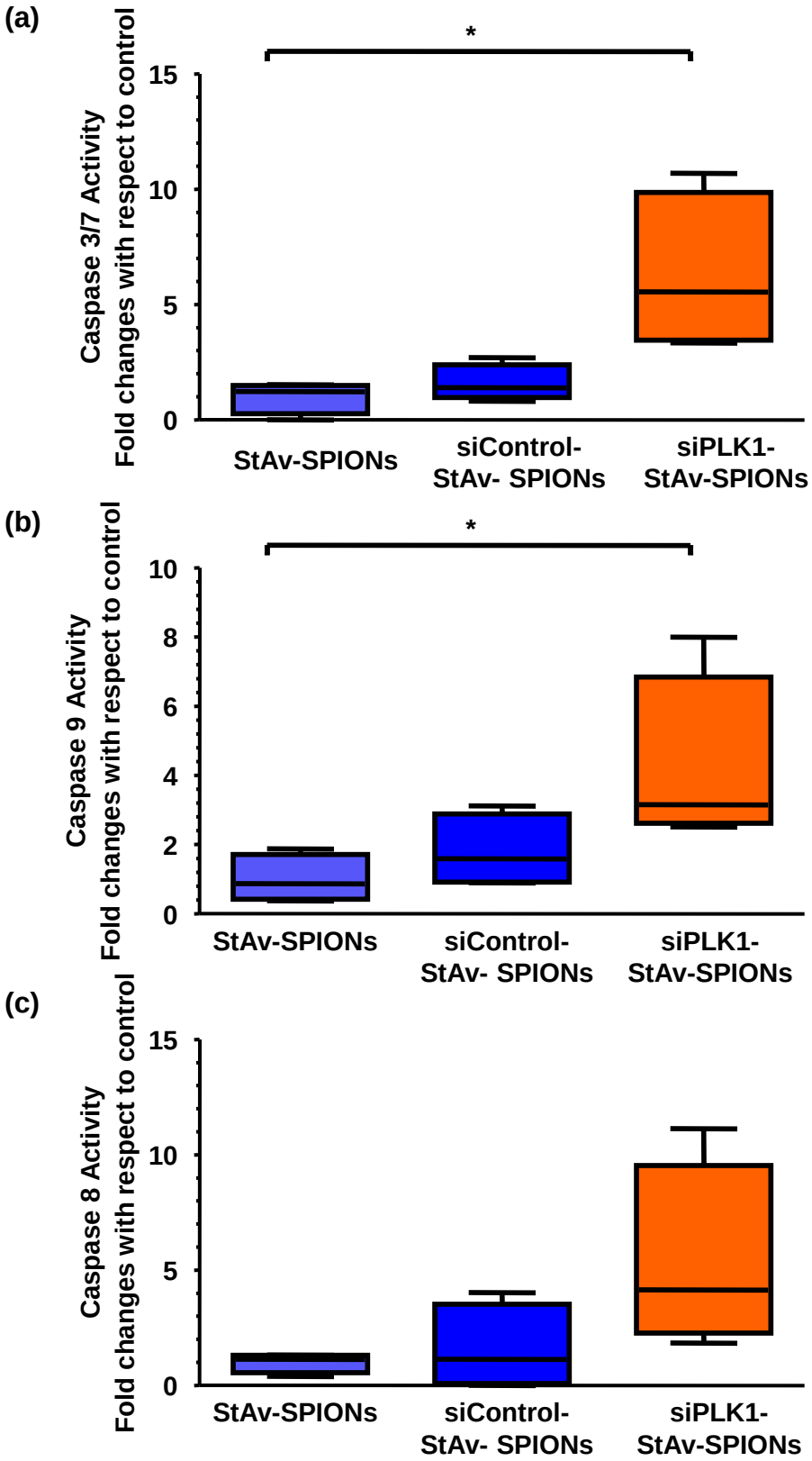

FIGURE S24: Influence of siPLK1-StAv-SPIONs treatment on caspase activity cascade in KPC mice. Caspase 3/7 (a), caspase 9 (b) and caspase 8 (c) activity in tumor tissue harvested from KPC mice of different treatment groups was measured using the flourogenic substrates R110-DEVD (caspase 3/7), AMC-IETD (caspase 8) and R110-LETD (caspase 9) (n=4-5 animals). *p<0.05 considered statistically significant.

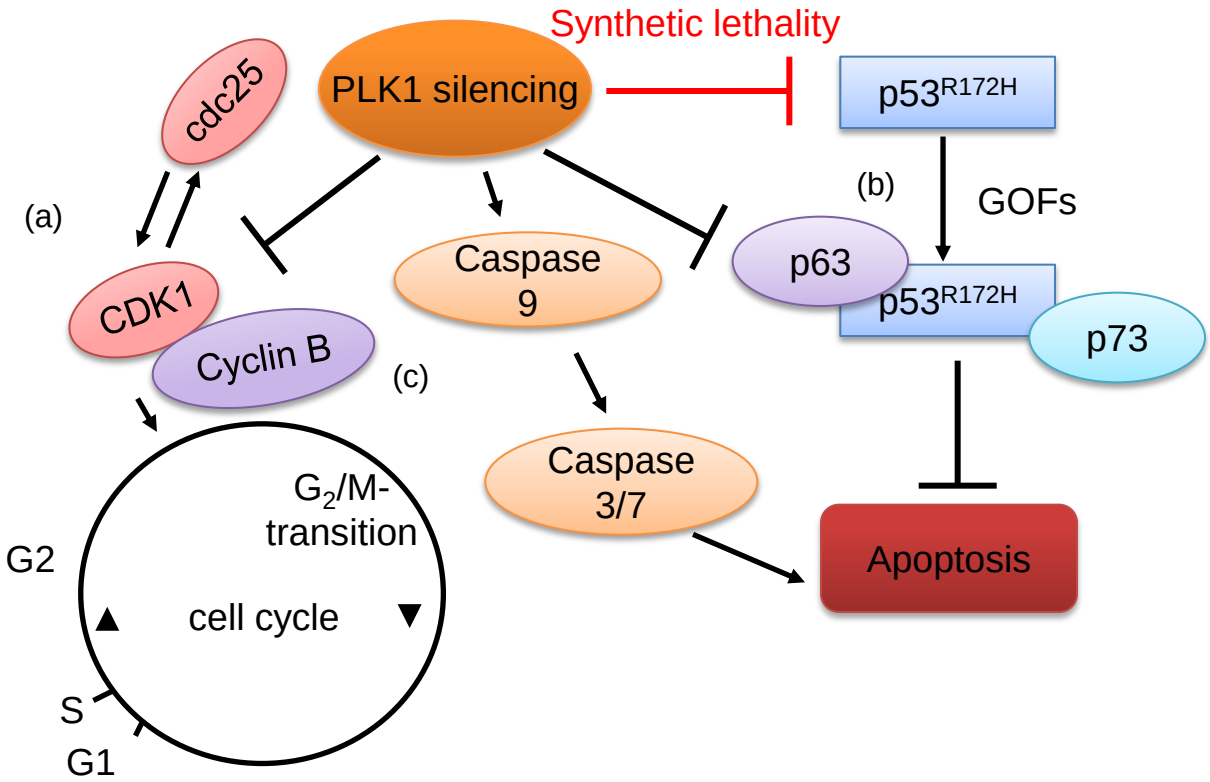

FIGURE S25: Possible mechanism of enhanced apoptosis on PLK1 silencing on siPLK1-StAv-SPIONs treatment. (a) PLK1 silencing mediates the downstream decrease in nuclear cdc25 localisation and subsequent nuclear CDK1/2 localisation, leading to a decrease in proliferation. PLK1 silencing leads to mitotic arrest as evident by accumulation of pHH3 and pericentrin again contributing to a decrease in proliferation [1]. Mitotic arrest is critically required for PLK1 silencing induced apoptosis. (b) $p53^{R172H}$ represents a gain of function (GOFs) mutation binding to phospho-p63 and p73 sub-units and thus reduces apoptosis. PLK1 silencing induces synthetic lethality by decreasing expression of $p53^{R172H}$. Moreover, PLK1 silencing by decreasing phosphorylation of p63 inhibits its binding to $p53^{R172H}$ and increases apoptosis [2-4]. (c) PLK1 silencing leads to caspase activation leading to apoptotic cell death execution by triggering cleavage of caspase 9 and caspase 3, whereas there are only minor effects on caspase 8 activation. PLK1 silencing induces the caspase dependent mitochondrial apoptotic pathway [5].

[1] Louwen et al. Oncotarget 2013
[2] Iwakuma et al. Oncogene 2007
[3] Gurpinar et al. Trends in Cell Biology 2015
[4] Müller et al Cancer Cell 2014
[5] Hugle et al. Cell Death and Differentiation,2015

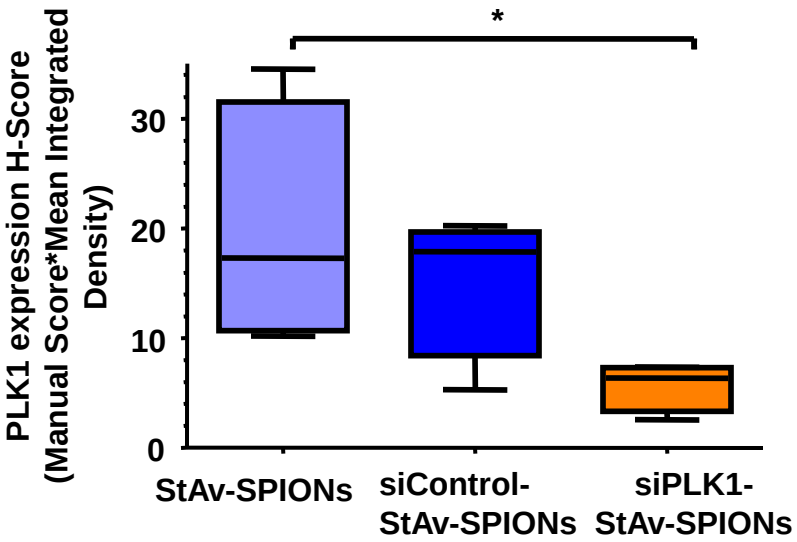

FIGURE S26: Change in PLK1 expression in KPC mice upon siPLK1-StAv-SPION treatment. After 2 weeks of siPLK1-StAv-SPIONs treatment, tumor showed significant reduced PLK1 expression if compared to controls. * $p<0.05$ considered statistically. (n=4)

(a)

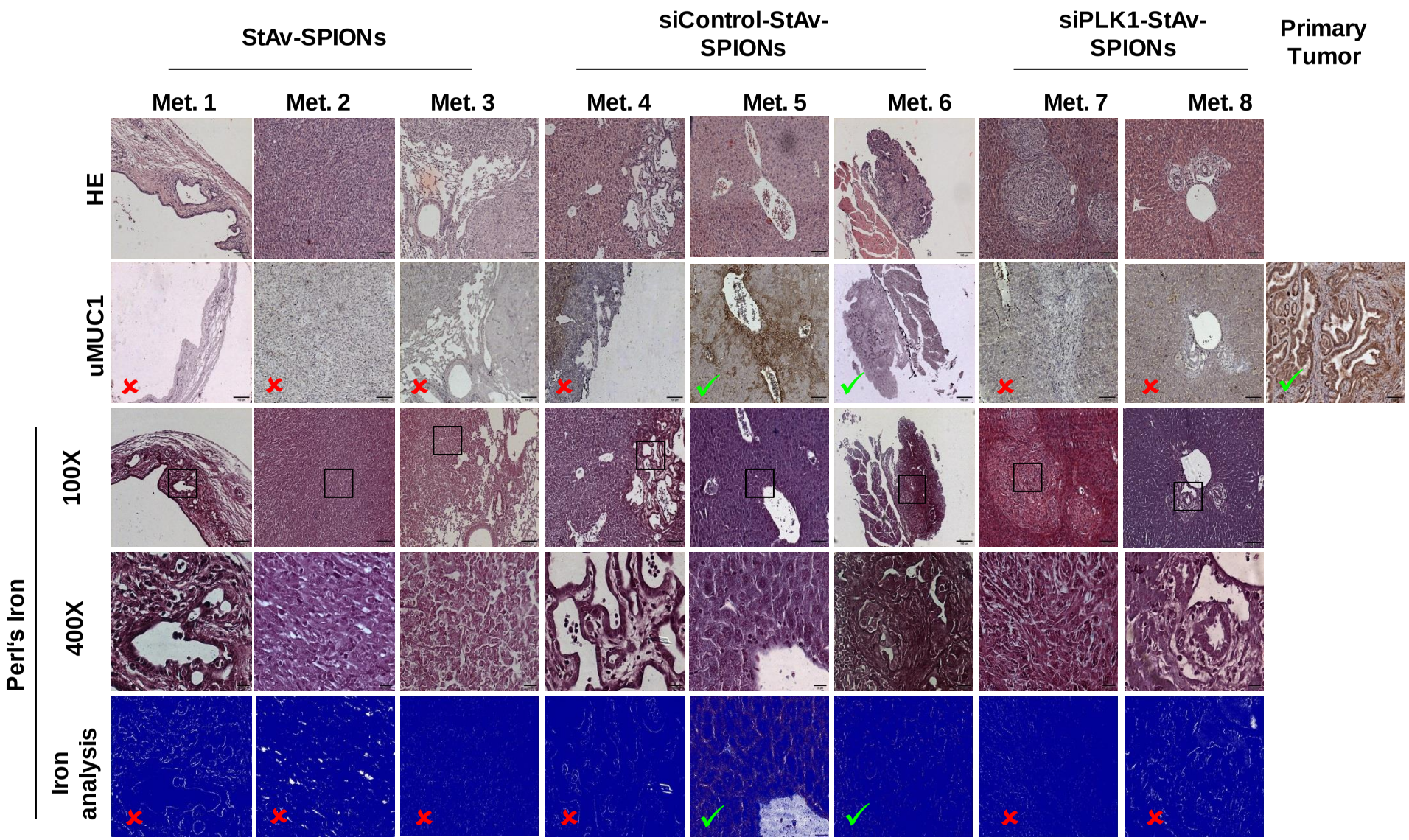
StAv-SPIONs
siControl-StAv-SPIONs
siPLK1-StAv-SPIONs
Primary Tumor
Met. 1
Met. 2
Met. 3
Met. 4
Met. 5
Met. 6
Met. 7
Met. 8
HE
uMUC1
Perl's Iron
100X
400X
Iron analysis

(b)

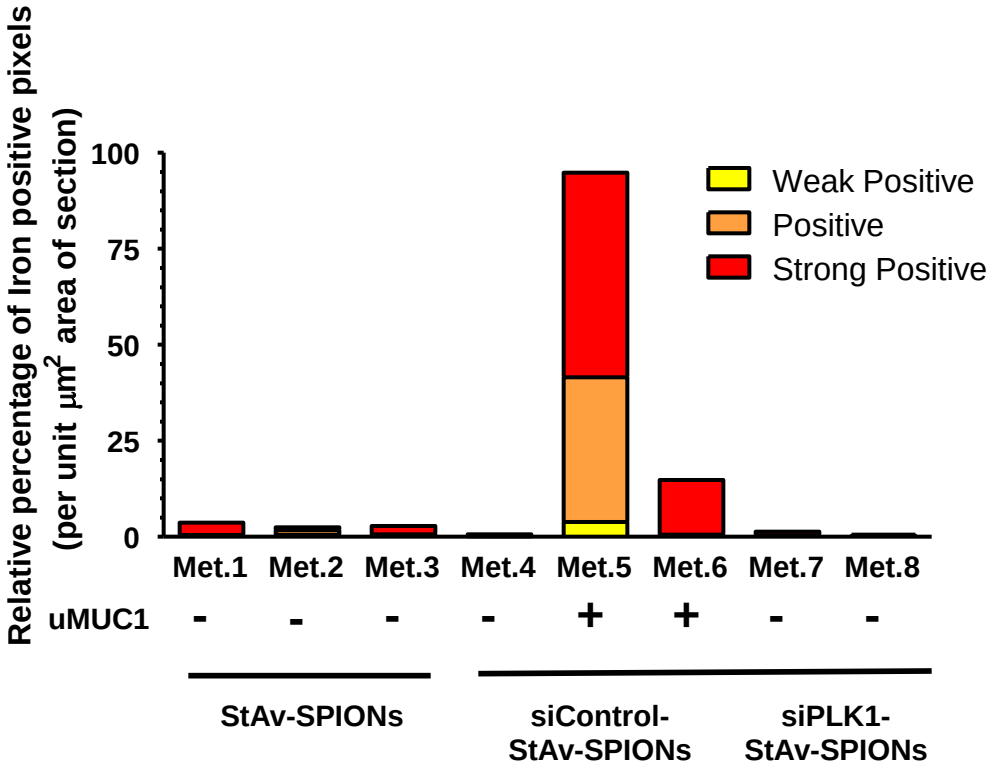

FIGURE S27: siPLK1-StAv-SPIONs uptake in metastatic and micro-metastatic tissues is associated with uMUC1 expression. (a) Representative metastatic tissues from different treatment groups and corresponding uMUC1 expression and iron staining on consecutive sections. Metastatic tissues which show uMUC1 expression correlated with iron uptake (✓ marked images). (b) Quantification of SPIONs uptake analysed by Aperio ImageScope software showed significant iron uptake in metastatic tissues that showed uMUC1 expression.

(a)

GFP fluorescence

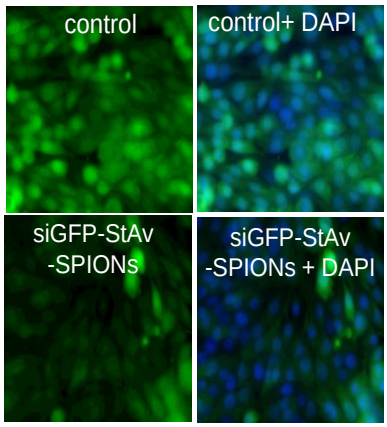

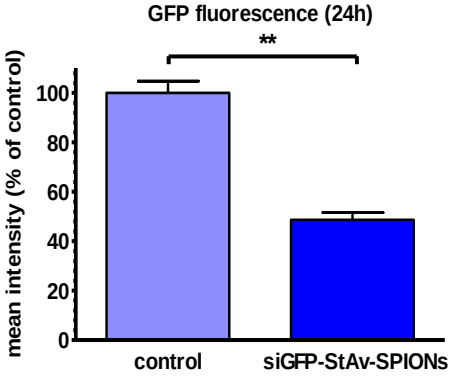

(c)

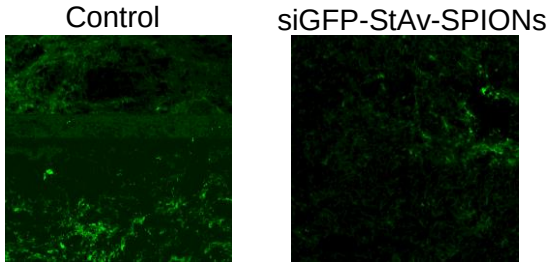

(b)

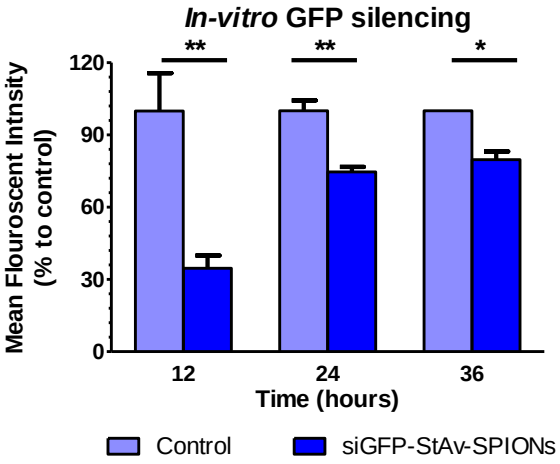

(d)

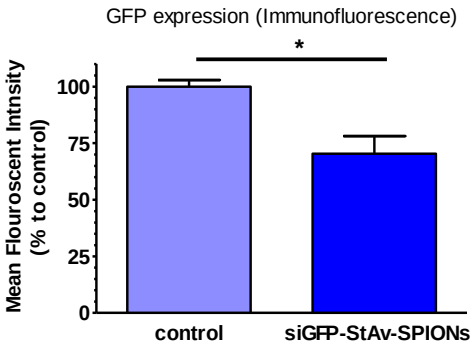

(e)

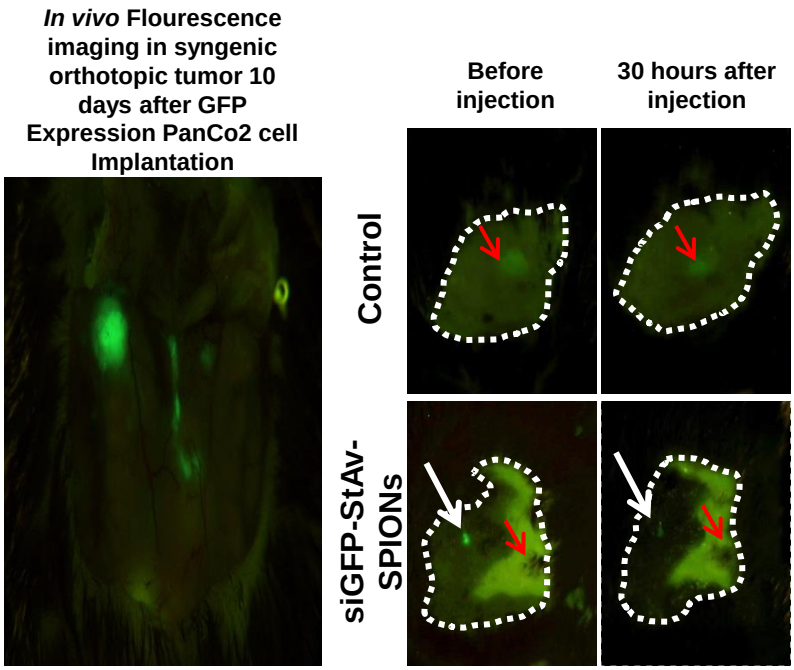

<u>Figure 28:</u> Influence of siGFP-StAv-SPIONs on GFP expressing PanCo2 cells (PanCo2G*) in vitro* and syngenic orthotopic tumor model *in vivo*. (a-b) PanCo2 G cells treated with siGFP-StAv-SPIONs showed time dependent silencing in GFP expression corresponding to control. (c-d) *In vivo* Syngenic orthotopic tumor model showed significant downregulation in GFP fluorescence, GFP expression 30 hours after treatment of siGFP-StAv-SPIONs (5mg/kg of iron, *i.v.*). (E) *In vivo* fluorescence imaging in syngenic orthotopic tumor 10 days after GFP expressing PanCo2 cells showed marked detectable fluorescence in vivo. 30 hours after siGFP-StAv-SPIONs treatment animals harboring PanCo2G tumor showed marked decrease compared to corresponding control. Area dipicted by red arrow indicates necrotic tumor.